JCTC Journal of Chemical Theory and Computation

Article

pubs.acs.org/JCTC

On the Innocence of Bipyridine Ligands: How Well Do DFT Functionals Fare for These Challenging Spin Systems?

Petr Milko and Mark A. Iron*

Computational Chemistry Unit, Department of Chemical Research Support, Weizmann Institute of Science, Rehovot, Israel 76100

Supporting Information

ABSTRACT: The electronic structures of a number of iron, cobalt, vanadium, and titanium complexes with the 2,2′-bipyridine (bpy) ligand were considered using the multireference CASSCF and NEVPT2 methods. Many of these systems have been studied in the past using B3LYP and were then found to contain the bpy ligand as a radical anion. For many of the cases, this is contradicted by our multireference calculations. While there are instances where the ligand is indeed a radical anion, in many cases it remains neutral and is involved in backbonding from the metal center. For those cases where CASSCF is too costly, a number of DFT functionals, including the newer double-hybrid functionals, were evaluated against the CASSCF data. It was found that nonhybrid functionals, especially those containing the kinetic energy density τ, were the best at predicting the electronic nature of the complexes. The τ-HCTH and HCTH functionals were the top performers, correctly predicting eleven out of eleven test cases and with the lowest mean unsigned errors (MUE, 7.6 and 7.8 kcal·mol^{-1}, respectively); the M06-L, N12, BLYP, PBE, and TPSS functionals also did well, while B3LYP had significant problems.

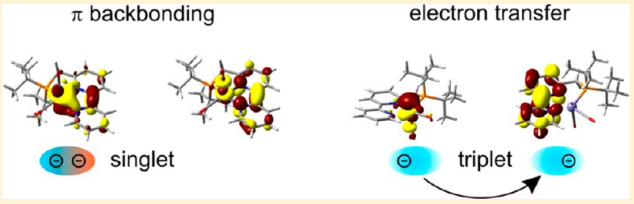

INTRODUCTION

The importance of transition metal complexes in the various fields of chemistry, including catalysis and metalloenzymes, needs not be established. One of the more commonly used ligands is 2,2′-bipyridine (bpy, see Scheme 1 for all ligands in this study). Complexes of this ligand and its derivatives are known for all the transition metals, and many important catalysts based on bpy are available. In many cases, the bpy ligand is just a spectator and does not have any direct chemical role in the reaction.

While traditionally ligands have just been spectators in a reaction, lately Milstein and co-workers have been developing a series of catalysts where the ligand is not innocent and plays a key role in catalysis, a process they termed metal−ligand cooperation (MLC). Their catalyst, ($^{t\mathrm{Bu}}$PNP*)Ru(H)(CO) ($^{t\mathrm{Bu}}$PNP = 2,6-*bis*(di-*tert*-butylphosphinomethyl)pyridine, the asterisk denotes a dearomatized ligand where one of the "arm" (exocyclic) methylene groups is deprotonated) and related complexes have been found to be efficient green catalysts for a wide variety of reactions,[1] including the dehydrogenative coupling of alcohols to esters,[1g,z] the dehydrogenative coupling of alcohols and amines to amides,[1i,s] and the hydrogenation of urea derivatives to methanol and the corresponding amine.[1q] The Milstein catalyst has also been shown to undergo other remarkable transformations, such as the reversible binding of CO_2,[2] aldehydes,[3] other carbonyl compounds,[4] and nitriles[5] that involve the reversible formation of C−C bonds. While much of the focus of homogeneous catalysis over the years has been on the second and third row transition metals, there has lately been a shift in focus to the first row metals. One distinct advantage is their significantly lower cost. For example, Milstein and co-workers have focused on pincer complexes of iron,[1u,ad,6] cobalt,[7] and nickel.[2c]

Likewise, there are cases in which the bpy ligand is not innocent. Under certain circumstances, it can show redox activity by accepting an electron to become a radical anion (i.e., bpy$^{\bullet-}$) or even a dianion (i.e, bpy^{2-}). This is another class of ligand participation: electron (or charge) transfer (i.e., ET or CT). For example, Irwin et al. showed, both computationally and experimentally using Mössbauer spectroscopy, that the iron(II) complex (bpy)Fe$^{\mathrm{II}}$(Mes)$_2$ (Mes = 2,4,6-mesityl) is reduced by potassium metal to give [(bpy$^{\bullet-}$)Fe$^{\mathrm{II}}$(Mes)$_2$]$^-$, an electron transfer (ET) state, rather than the expected non-ET [(bpy)Fe$^{\mathrm{I}}$(Mes)$_2$]$^-$.[8] Here the iron and bpy ligand play "hot potato" to see who would rather have/not have the extra electron.

Recently, Scarborough and Wieghardt computationally examined a series of bpy transition metal complexes, including (bpy)Fe(η^6-toluene), and concluded that the observed shortening of the $C_2-C_{2'}$ bond (i.e., the bond between the two pyridine moieties in bpy) in X-ray crystallography results from formation of a (bpy$^{\bullet-}$)Fe$^{\mathrm{I}}$(η^6-toluene) complex,[9] rather than the extensive π-backbonding suggested by Radanovich et al.[10] Our interest in such systems began with Milstein and co-workers' synthesis of (R_2PCH_2bpy)Fe(CO)$_2$ (**1**, R_2PCH_2bpy = 6-(dialkylphosphinomethyl)-2,2′-bipyridine, alkyl (R) = *tert*-butyl, *iso*-propyl or phenyl). They observed a similar shortening of the $C_2-C_{2'}$ bond in their complexes and were curious about the electronic structure of the complexes.[6e] Using computa-

Received: October 21, 2013

   dx.doi.org/10.1021/ct400913z | J. Chem. Theory Comput. XXXX, XXX, XXX−XXX

Scheme 1. Ligands in This Study

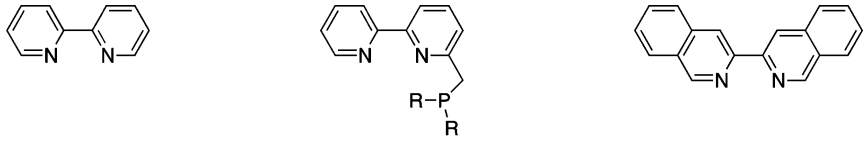

2,2'-bipyridine (bpy) 6-(dialkylphosphinomethyl)-2,2'-bipyridine (R_2PCH_2bpy) 2,2'-biquinoline (bq)

tional methods is becoming more commonplace as experimentally determining the electronic structure of complexes is difficult and often inconclusive.

In (bpy)$Fe^0(\eta^6$-toluene), one has an iron(0) center, which is a common and stable oxidation state for iron, and a neutral bpy ligand, which corresponds to "conventional" coordination chemistry rules. On the other hand, in the postulated ($bpy^{\bullet-}$)$Fe^I(\eta^6$-toluene), one would have both an iron(I) center—which would rather accept or give up one electron—and the $bpy^{\bullet-}$ radical anion—which would prefer to relinquish one electron; thus, it would be natural for the system to revert to the nonelectron transfer state. The situation is different for the reduction product of (bpy)$Fe^{II}(Mes)_2$: one has either an unstable Fe^I or an unstable $bpy^{\bullet-}$ radical anion, which results in a balance between these two unfavorable situations, in this case favoring the radical anion.

In their computational investigations of (bpy)Fe(η^6-toluene) and a selection of other complexes, Scarborough, Wieghardt and co-workers used the B3LYP exchange-correlation functional.[9,11] One complication of using these lighter first-row transition metals is their tendency of adopting different spin states depending on their ligand environment (and can even depend on temperature or solvent, but this is far beyond the scope of this paper). Thus, one needs a reliable, yet easy and cost-effective, method of evaluating the spin state of any given complex. For many years, "reliable yet easy and cost effective" has meant density functional theory (DFT). Before applying the same methodology to our system, we wanted to confirm its applicability. In (bpy)Fe(η^6-toluene), the biradical would be formed by ET from the metal to the ligand, and the resulting open-shell singlet state of such a species cannot be adequately described by less than two Slater determinants (reference states). DFT is a single-reference methods and thus may be inappropriate for this case.

Because of these concerns, we decided to first evaluate the performance of the previously applied methodology. The CASSCF (complete active space self-consistent field) method is a reliable, albeit computationally very demanding, method for evaluating systems suspected of having significant multireference character; these results can further be improved by adding a second-order perturbation theory approach to the CASSCF wave function (we specifically chose the *n*-electron valence state perturbation theory—NEVPT2—approach). We find that depending in the specific complex at hand, both situations, that is π-backbonding and ET, are observed.

Equally important to the chemistry of a complex is identifying a reliable method to evaluate said chemistry. Toward this end, we evaluated a large number of DFT methods. On the basis of the CASSCF and NEVPT2 results, which are presented herein, we show that hybrid DFT exchange-correlation functionals (such as B3LYP) fail for many of these systems and are thus inapplicable. We also considered the newer double-hybrid functionals,[12] which include a fraction of MP2-like correlation; these methods have a fraction of the cost of CASSCF, are much more user-friendly, and have been shown to be very reliable in many instances.[13] Nonetheless, these too were found to be inappropriate for the problems considered here. Surprisingly, the older GGA and meta-GGA functionals do quite well in predicting the spin states and excitation energies of our test set of complexes.

COMPUTATIONAL METHODS

All calculations used either GAUSSIAN09 Revisions C.01 and D.01[14] or ORCA 2.9.0;[15,16] double hybrid DFT single point energies and CASSCF/NEVPT2 calculations were done using the latter while hybrid DFT (and some double hybrid calculations) were done with the former.

Geometries of complexes **1a–c** were optimized using the M06 DFT hybrid functional,[17−21] which is the hybrid variant of Truhlar's Minnesota-06 suite of functionals and has 27% exact exchange.[22] The geometries of the other complexes were taken from previous studies,[6d,8,9] as were the CASSCF and NEVPT2 results for complex **9**.[6d]

Complete active space self-consistent field (CASSCF)[23] and *n*-electron valence state perturbation theory (NEVPT2)[24] calculations were performed using the M06 optimized geometries. The geometries of complexes **1a–c** were optimized using the M06 functional with the SDD(d) basis set-relativistic effective core potential (RECP) combination, which combines the Stuttgart-Dresden basis set-RECP on transition metals,[25] the Dunning–Huzinaga double-ζ plus polarization functions (D95(d,p)) basis set on the main group elements.[26] Singlet, triplet, and quintet (or, where appropriate, doublet, quartet, and sextet) states were considered. MP2 natural orbitals were generated as the guess for the CASSCF calculations. The natural orbitals containing the transition metal *d* functions were selected as the initial active space. After preliminary CASSCF calculations, the active space was reduced by removing orbitals with CASSCF orbital occupancies very close to 2 or 0, as recommended by the ORCA manual; occupancies of approximately 2 or 0 indicate that excitation to or from these orbitals does not contribute to the CASSCF wave function and their inclusion in the active can cause convergence problems. Table 1 lists the final active spaces of all complexes studied

Table 1. Number of Orbitals (n_{orb}) and Electrons (n_{el}) in the Active Spaces of the Complexes Studied

	n_{orb}	n_{el}		n_{orb}	n_{el}
[(tBu-NNP)Fe(CO)$_2$] (**1a**)	12	12	[(η^5-Cp)Co(bpy)] (**4**)	10	10
[(iPr-NNP)Fe(CO)$_2$] (**1b**)	12	12	[(η^5-Cp)(η^3-Cp)V(bpy)] (**5**)	10	9
[(Ph-NNP)Fe(CO)$_2$] (**1c**)	12	12	[(η^5-Cp)$_2$Ti(bpy)] (**6**)	10	10
[(mes)$_2$Fe(bpy)] (**2**)	8	9	[(η^5-Cp*)$_2$Ti(bpy)] (**7**)	10	10
[(tol)Fe(bpy)] (**3**)	10	10	[(η^5-Cp)$_2$Ti(bq)] (**8**)	12	12

dx.doi.org/10.1021/ct400913z | J. Chem. Theory Comput. XXXX, XXX, XXX–XXX

here. The efficiency of the calculation was improved by using the resolution of identity chain of spheres (RIJCOSX) approximation.[27]

All energy calculations, whether in ORCA or GAUSSIAN09, used the def2-SVP and def2-TZVPP basis sets, which are respectively double-ζ and triple-ζ quality basis sets with one and two sets of polarization functions;[28] they include a relativistic effective core potential (RECP) on second and third row transition metals.[29] The basis sets for GAUSSIAN09 were taken from the EMSL Basis Set Exchange,[30] while in ORCA they are built-in. CASSCF and NEVPT2 calculations used the def2-TZVPP basis set, except for complexes **7** and **8** where the def2-SVP basis set was used due to the large size of the system. In the evaluation of the various DFT functionals (Tables 13 and 14), the def2-SVP basis set was used.

In addition, a number of the newer functionals from the Truhlar group were considered:[31]

- M11:[32] the hybrid meta-GGA (mGGA) exchange-correlation functional of the Minnesota-11 suite
- M11-L:[33] the local (nonhybrid) variant of M11
- MN12-L:[34] the local meta-nonseparable gradient approximation (mNGA) exchange-correlation functional of the Minnesota-12 suite
- M12SX:[35] Truhlar's range-separated hybrid (RSH) member of the Minnesota-12 suite of functionals with 25−0% screened exchange
- N12:[36] Truhlar's 2012 NGA exchange-correlation functional
- N12-SX:[35] Truhlar's RSH variant of N12 with 25−0% screened exchange

For completeness, a few more conventional functionals were assessed, namely:

- B3LYP: Becke's three-parameter hybrid functional[19] with 20% "exact" Hartree−Fock exchange with the Becke-88 (B88) exchange[20] and the Lee−Yang−Parr (LYP) correlation[21]
- BLYP: the nonhybrid version of B3LYP with B88 exchange and LYP correlation
- PBE:[37] the Perdew−Burke−Ernzerhof (PBE) exchange-correlation functional
- PBE0:[38] Adamo and Barone's hybrid version of PBE with 25% "exact" Hartree−Fock exchange
- M06:[18] vide supra
- M06-L:[39] the local variant of M06
- APFD: the Austin−Frisch−Petersson functional with dispersion, a hybrid functional with 23% exact exchange
- HCTH:[40] the "407" version of the Hamprecht−Cohen−Tozer−Handy GGA functional
- τ-HCTH:[41] Boese's meta-GGA version of HCTH
- τ-HCTHhyb:[41] Boese's hybrid version of τ-HCTH
- BMK:[42] Boese and Martin's τ-dependent hybrid functional parametrized for kinetics
- B1B95:[43] Becke's one parameter hybrid functional with B88 exchange and Becke-95 (B95)[43] τ-dependent correlation functional
- TPSS:[44] Tao, Perdew, Staroverov, and Scuseria's τ-dependent GGA functional (Note: these calculations were run using ORCA)

A number of double hybrid functionals were evaluated. These functionals include, in addition to a percentage of exact Hartree−Fock exchange, a percentage of "Møller−Plesset"-like correlation. The functionals chosen are the following:

- B2PLYP: Grimme's original double hybrid functional with B88 exchange and LYP correlation[45]
- B2GP-PLYP, B2K-PLYP, and B2T-PLYP: Martin and co-workers' reparameterization of Grimme's B2PLYP functional for general purpose, kinetics and thermodynamics, respectively[46]
- PWPB95: Goerigk and Grimme's double hybrid functional with reparameterized Perdew−Wang-91 (PW) exchange[47] and B95[43] correlation functionals[48]
- Kozuch and Martin's dispersion corrected (they include an empirical dispersion correction[49]—specifically Grimme's third version of his empirical dispersion correction (DFTD3)[49a,50] with Becke−Johnson (BJ) dampening[50,51]), spin component scaled (i.e., an SCS[52]-MP2[53]-like correlation contribution), double hybrid (DSD) functionals, specifically
  - DSD-BLYP: the original DSD functional incorporating the B88 exchange and LYP correlation functionals[54]
  - DSD-PBEP86: a reparameterization using the Perdew-Burke-Ernzerhof (PBE)[37] exchange and Perdew-86 (P86)[55] correlation functionals[56]
  - DSD-PBEhB95: the latest in the series incorporating the 1998 revision of the PBE exchange (i.e., PBEh)[57] and the B95[43] correlation functional.[58] (Note: For technical reasons (lack of functionality in ORCA), the PBE exchange functional was used in lieu of the PBEh functional; it can be shown that for chemical properties, the difference between the two exchange functionals is very small, especially considering that in the double hybrid functional one has a large amount of Hartree−Fock exchange, and one can substitute one for the other.[59]) (Note: Because the release version of ORCA used throughout the paper lacks the B95 correlation functional, these calculations were performed using an alpha version of ORCA 3.0 (3450) kindly provided to Prof. Martin (Weizmann Institute of Science) by Frank Wennmohs.)

When using a DFT method, extended Hückel theory (EHT) orbitals were used as the initial guess for all energy calculations. In order to obtain the open-shell singlet states, the optimized triplet orbitals were used as the starting guess for an unrestricted Kohn−Sham (or Hartree−Fock for SCS-MP2) calculation.

RESULTS AND DISCUSSION

The electronic structures of $(R_2PCH_2bpy)Fe(CO)_2$ (R = ^{t}Bu−**1a**, ^{i}Pr−**1b**, or Ph−**1c**) were considered at various levels of theory. Beyond doubt, the NEVPT2 results are the most reliable (Table 2). The twelve CASSCF optimized orbitals used to build the configuration state functions (CSFs) are shown in Figure 1, and the occupation numbers of each natural orbital in each of the four CSFs (ψ_{1-4}) of particular interest are shown in Table 3.

From these results, an examination of the wave function of the ground state shows that it is clearly a closed-shell singlet. Two MOs are key to understanding the electronic state of the complexes (blue box in Figure 1): a bonding φ_6 (σ with respect to the metal center and the two nitrogen atoms of the bpy component of the ligand) and an antibonding φ_7 (σ^*) mixing of an iron d_{z^2} and LUMO of the ligand. The contributions of

dx.doi.org/10.1021/ct400913z | J. Chem. Theory Comput. XXXX, XXX, XXX−XXX

Table 2. CASSCF(12,12)/TZVPP and NEVPT2/TZVPP Relative Energies (kcal·mol^{-1}) of the M06/SDD(d) Optimized [$(R_2PCH_2bpy)Fe^0(CO)_2$] Complexes

complex	electronic state	ΔE^{CASSCF}	ΔE^{NEVPT2}	ΔG^{CASSCF}	ΔG^{NEVPT2}
1a	S[a]	0.0	0.0	0.0	0.0
	S[b]	−1.8	3.3	−2.4	2.7
	T[c]	8.7	28.3	5.7	25.4
	Qi[d]	16.1	54.5	8.9	47.4
1b	S[a]	0.0	0.0	0.0	0.0
	S[b]	−0.2	2.9	−1.3	1.9
	T	11.2	26.0	8.7	23.5
	Qi	1.8	51.1	−6.9	42.4
1c	S[a]	0.0	0.0	0.0	0.0
	T	−1.6	23.3	−6.5	18.5
	Qi	8.3	50.7	0.1	42.5

[a]The structure was optimized as a closed-shell singlet at the RM06/SDD(d) level of theory. [b]The structure was optimized as an open-shell singlet at the UM06/SDD(d) level of theory. [c]Triplet state. [d]Quintet state.

each CSF to the CASSCF wave function are given in Table 4, and the CASSCF orbital occupancies are given in Table 5. The orbital compositions of the key MOs (vide infra) of all complexes in this study, are listed in Table 6. The closed-shell contribution (i.e., ψ_1) is dominant in the singlet state with nearly 80% weight, while the second most dominant CSF is the other closed shell ψ_2; thus, these complexes are best described as closed-shell singlets with an iron(0) center and a neutral bpy ligand. This is also reflected in the MO occupancies where the HOMO has nearly 2e$^-$. The HOMO for **1** (*i.e.*, φ_6), as noted above, is a bonding interaction between the metal and the ligand, known as metal−ligand backbonding akin to that commonly observed for transition metal carbonyl complexes (c.f., MOs $\boldsymbol{\varphi}_3$−$\boldsymbol{\varphi}_5$).

Table 3. CSF Occupancies of Important CSFs for the CASSCF(12,12) for Complexes 1a−c[a]

	MO (φ) in CSF											
	1	2	3	4	5	**6**	**7**	8	9	10	11	12
ψ_1	2	2	2	2	2	**2**	**0**	0	0	0	0	0
ψ_2	2	2	2	2	2	**0**	**2**	0	0	0	0	0
ψ_3	2	2	2	2	2	**1**	**1**	0	0	0	0	0
ψ_4	2	2	2	2	**1**	**1**	**1**	**1**	0	0	0	0

[a]In bold are the key MOs of interest.

Table 4. Individual CSF Contributions (Square of the CSF Expansion Coefficients) to the CASSCF Wavefunction for Complexes 1a−c

	electronic state	ψ_1	ψ_2	ψ_3	ψ_4
1a	S[a]	0.7820	0.0575	<0.01[c]	
	S[b]	0.7486	0.0996	<0.01	
	T			0.8657	<0.01
	Qi				0.8581
1b	S[a]	0.7929	0.0460	<0.01	
	S[b]	0.7510	0.0970	<0.01	
	T			0.8655	<0.01
	Qi				0.7965
1c	S[a]	0.7920	0.0494	<0.01	
	T			0.8675	<0.01
	Qi				0.8693

[a]The structure was optimized as a closed-shell singlet at the RM06/SDD(d) level of theory. [b]The structure was optimized as an open-shell singlet at the UM06/SDD(d) level of theory. [c]Value below threshold of 0.01 for printing result in electronic structure code (ORCA).

Furthermore, if one compares the geometries of **1b** optimized using M06 as a closed-shell (RKS) and an open-shell (UKS) singlet with the X-ray structure, one notes that

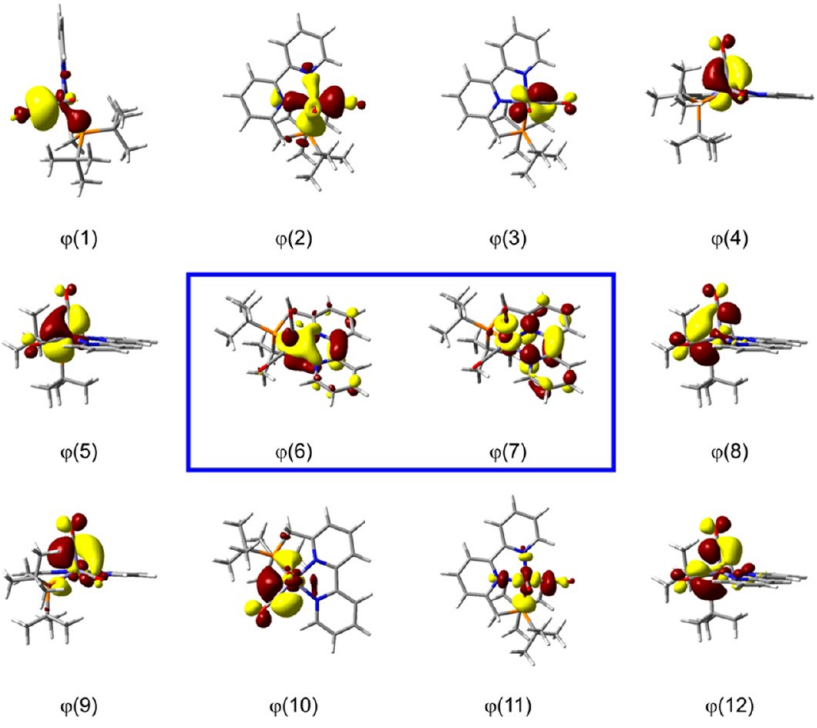

Figure 1. CASSCF(12,12) active orbitals for complex **1a**. Those for **1b** and **1c** are very similar (see the Supporting Information, Figures S3−S4).

dx.doi.org/10.1021/ct400913z | J. Chem. Theory Comput. XXXX, XXX, XXX−XXX

Table 5. CASSCF Orbital Occupancies for Complexes 1a−c

		MO (φ)											
	electronic state	1	2	3	4	5	**6**	**7**	8	9	10	11	12
1a	S[a]	1.98	1.95	1.93	1.91	1.91	**1.80**	**0.19**	0.09	0.08	0.06	0.05	0.02
	S[b]	1.98	1.96	1.93	1.92	1.91	**1.72**	**0.28**	0.08	0.08	0.06	0.05	0.02
	T	1.99	1.96	1.93	1.92	1.92	**1.00**	**0.99**	0.08	0.07	0.06	0.05	0.02
	Qi	1.99	1.99	1.90	1.88	1.00	**1.00**	**0.99**	0.99	0.11	0.10	0.01	0.01
1b	S[a]	1.98	1.95	1.93	1.92	1.90	**1.83**	**0.16**	0.09	0.07	0.06	0.06	0.03
	S[b]	1.98	1.96	1.93	1.92	1.91	**1.72**	**0.27**	0.08	0.08	0.06	0.05	0.02
	T	1.99	1.96	1.93	1.93	1.92	**1.00**	**0.99**	0.08	0.07	0.06	0.05	0.02
	Qi	1.96	1.95	1.87	1.86	**1.00**	**1.00**	**1.00**	**1.00**	0.15	0.13	0.05	0.03
1c	S[a]	1.98	1.95	1.93	1.92	1.90	**1.82**	**0.17**	0.09	0.07	0.06	0.05	0.03
	T	1.99	1.96	1.94	1.93	1.92	**1.00**	**0.99**	0.08	0.07	0.06	0.05	0.02
	Qi	1.99	1.99	1.91	1.89	1.01	**1.00**	**0.99**	0.99	0.11	0.08	0.01	0.01

[a]The structure was optimized as a closed-shell singlet at the RM06/SDD(d) level of theory. [b]The structure was optimized as an open-shell singlet at the RM06/SDD(d) level of theory.

Table 6. Formal Oxidation State of the Metal Center (M) and the bpy-Based Ligand (L) and Composition of the Key Molecular Orbitals

		oxidation state		$\varphi(i)$		$\varphi(j)$	
complex	electronic state	M	L	M	L	M	L
1a	CS-S[a]	0	0	57.6 (d_{z^2} + d_{yz})	34.2	44.2 (d_{z^2} + d_{yz})	47.7
	OS-S[b]	0	0	53.8 (d_{z^2} + d_{yz})	38.2	41.4 (d_{z^2} + d_{yz})	50.8
	T	I	−I	2.5 (d_{z^2} + d_{yz})	92.5	83.0 (d_{z^2} + d_{yz})	4.8
1b	CS-S[a]	0	0	57.9 (d_{z^2} + d_{xz} + $d_{x^2-y^2}$)	30.2	43.9 (d_{z^2} + d_{xz} + $d_{x^2-y^2}$)	44.9
	OS-S[b]	0	0	53.6 (d_{xz})	38.1	41.0 (d_{xz})	51.3
	T	I	−I	2.1 (d_{xy} + d_{yz})	92.7	84.3 (d_{xy} + d_{yz})	5.4
1c	CS-S[a]	0	0	57.5 (d_{z^2})	31.1	44.0 (d_{z^2})	46.8
	T	0	0	2.7 (d_{z^2})	93.1	84.1 (d_{z^2})	6.0
2	Qa	II	−I	51.3 (d_{xz})	45.4	45.7 (d_{xz})	50.6
	Se	II	−I	18.5 (d_{yz})	80.2		
3	S	0	0	56.0 (d_{yz})	41.0	48.5 (d_{yz})	46.0
	T	0	0	56.4 (d_{yz})	41.8	44.0 (d_{yz})	52.1
4	S	I	0	57.4 (d_{yz})	39.8	44.5 (d_{yz})	46.9
	T	II	−I	89.7 (d_{yz})	2.2	2.5 (d_{yz})	93.7
5	D	III	−I	50.8 (d_{xz})	43.6	44.8 (d_{xz})	52.0
	Qa	III	−I	74.2 (d_{xz})	20.2	22.3 (d_{xz})	74.3
6	S	III	−I	50.7 ($d_{x^2-y^2}$)	43.4	46.1 ($d_{x^2-y^2}$)	49.8
	T	III	−I	5.6 ($d_{x^2-y^2}$)	90.5	90.4 ($d_{x^2-y^2}$)	5.0
7	S	III	−I	50.6 ($d_{x^2-y^2}$)	43.4	46.9 ($d_{x^2-y^2}$)	49.0
	T	III	−I	27.5 ($d_{x^2-y^2}$)	61.3	69.6 ($d_{x^2-y^2}$)	24.3
8	S	III	−I	49.4 ($d_{x^2-y^2}$)	46.3	48.4 ($d_{x^2-y^2}$)	48.0
	T	III	−I	1.9 ($d_{x^2-y^2}$)	94.4	96.3 ($d_{x^2-y^2}$)	0.6

there is greater similarity with the RKS structure.[60] The X-ray and the RKS structures are both trigonal bipyramids, while the UKS structure is better described as square pyramidal (Figure 2). Likewise, from the bond angles listed in Table 7, clearly the angles for RKS are closer to the X-ray values than are the UKS angles. The deviations in the N−Fe−CO angles result from the experimentally observed fluxionality of the trigonal bipyrimidal complex between the two equivalent structures; heating or cooling during the ^{1}H NMR spectra measurements results in sharper signals as this either makes the equilibrium so fast or so slow on the NMR time scale that the complex appears as one unique signal.[6e] The structures of **1a** and **1c** cannot be compared in the same way as the RKS and UKS structures are more similar; in contrast to **1b**, the X-ray structures of these two complexes are square pyramidal.

Moreover, as noted in the Introduction, a biradical (i.e., open-shell singlet) situation does not even make chemical sense for **1a−c** or **3**. In these cases, one would have an iron(I) metal center and a bpy$^{\bullet-}$ radical anion. Neither is an ideal situation. The iron center would rather gain or lose one electron, while the radical anion would much rather lose its spare electron. In this situation, both components would be happier if the system were to revert to an iron(0) and a neutral bpy.

Another important geometric parameter is the $C_2-C_{2'}$ bond. Coordination of the bpy moiety to the metal center is accompanied by a shortening of this bond. This can be caused by either π-backdonation or single-electron transfer to the LUMO of the bpy moiety. While this bond is found by X-ray crystallography to be shorter in bpy$^{\bullet-}$ (1.431(3) Å) and bpy^{2-} (1.399(6) Å) than in bpy (1.490(3) Å),[61] Biner et al. have noted, at least for ruthenium complexes, that this bond length is not a reliable indicator of the oxidation state (i.e., formation of an ET species).[62] Inspection of the CASSCF orbitals shows that the key MOs contain a π bonding interaction on the bpy ligand between C_2 and $C_{2'}$. The partial occupation of this orbital in the CASSCF wave function results in a stronger, and hence shorter, $C_2-C_{2'}$ bond. It can thus be argued that this $C_2-C_{2'}$ bond shortening, at least in complexes **1**, is a result of coordination to the metal center and electron π-backdonation from the metal to the ligand.

In contrast to complexes **1**, [(bpy)Fe(Mes)$_2$]$^-$ (**2**) has significant bpy$^{\bullet-}$ character. The ground state, according to NEVPT2, is indeed a quartet (Qa), although the sextet (Se) state is only 4.2 kcal·mol^{-1} higher in energy (Table 8). Here, the two key MOs are φ_3 and φ_7 (Figure 3), both of which are metal−ligand overlap MOs. In this case, there are three CSFs that have significant, and roughly similar, contributions to the CASSCF wave functions (Table 9). Two of these CSFs have three unpaired electrons and either two or zero electrons in these key MOs; the third (ψ_3) has five unpaired electrons (by necessity four α and one β spins to maintain a quartet state)

dx.doi.org/10.1021/ct400913z | J. Chem. Theory Comput. XXXX, XXX, XXX−XXX

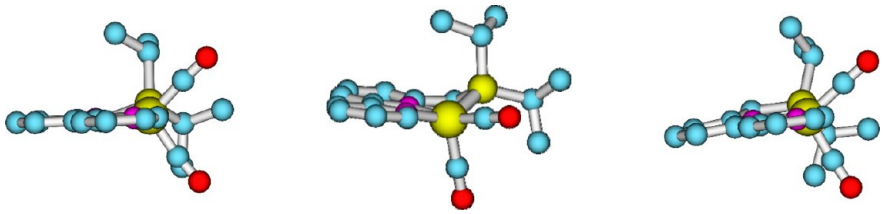

Figure 2. Comparison of the geometries of **1b** optimized with M06 as a closed-shell singlet (RKS, left) and as an open-shell singlet (UKS, middle) with the X-ray structure[6e] (right). Hydrogen atoms have been omitted for clarity.

Table 7. Comparison of the Geometries (Angles in Degrees) of 1b Optimized with M06 as a Closed-Shell (RKS) and an Open-Shell (USK) Singlet with the X-ray Structure

angle	RKS	UKS	X-ray[a]
N1−Fe−P	160.4	143.0	161.3
N2−Fe−C1O	131.4	166.2	141.1
N2−Fe−C2O	120.3	98.1	115.8
N2−Fe−P	83.2	81.0	84.0
N2−Fe−N1	80.3	80.3	80.4
C10−Fe−C20	102.3	95.4	103.1

[a]From ref 6e.

Table 8. CASSCF(9,8)/def2-TZVPP and NEVP2/def2-TZVPP Relative Energies (kcal·mol^{-1}) of $[(bpy)Fe^{I}(mes)_2]^-$ (2)

	ΔE_{CASSCF}	ΔE_{NEVPT2}
Qa[a]	0.0	0.0
Se[b]	2.4	4.2

[a]Quartet state. [b]Sextet state.

with one electron in each of these two MOs. As a result, the MO occupations (Table 10) clearly have five singly occupied MOs (again, clearly one electron has β spin), a situation also described by the B3LYP calculations of Irwin et al.,[8] although using (vide infra) the incorrect orbitals. Moreover, based on the NBO charges and Löwdin spin densities in this complex (Table 11), it would not be inaccurate to describe the bpy ligand in **2** as a radical anion.

Table 9. CSF Occupancies of CASSCF Orbital References for Complex 2 and Their Individual Weights (Square of the CSF Expansion Coefficients)

elctronic state		weight	1	2	3	4	5	6	7	8
Qa	ψ_1	0.4280	2	2	**2**	1	1	1	**0**	0
	ψ_2	0.2295	2	2	**0**	1	1	1	**2**	0
	ψ_3	0.3339	2	2	**1**	1	1	1	**1**	0
Se	ψ_4	0.9924	2	2	**1**	1	1	1	**1**	0

A number of additional complexes were examined using CASSCF and NEVPT2: (η^6-tol)Fe(bpy) (**3**, tol = toluene), (η^5-Cp)Co(bpy) (**4**, Cp = $C_5H_5^-$ cyclopentadienyl), (η^5-Cp)(η^3-Cp)V(bpy) (**5**), (η^5-Cp)$_2$Ti(bpy) (**6**), (η^5-Cp*)$_2$Ti(bpy) (**7**, Cp* = $C_5Me_5^-$ pentamethylcyclopentadienyl), (η^5-Cp)$_2$Ti(bq) (**8**, bq =2,2′-biquinoline, see Scheme 1); (^{i}Pr$_2$PCH$_2$bpy)FeCl$_2$ (**9**) was considered in a previous report[6d] and is included here in this discussion. The intent is to understand the electronic nature of the bpy ligand.

Complex **3** is very similar to complexes **1**. There was a discussion in the past about the nature of the shorting of the $C_2-C_{2'}$ bond in complex **3** and thus about its electronic structure. Radanovich et al. synthesized the complex and characterized it by X-ray crystallography.[10] They suggested based on spectroscopic data that the shorting of the $C_2-C_{2'}$ bond is caused by the extensive π-backbonding and the

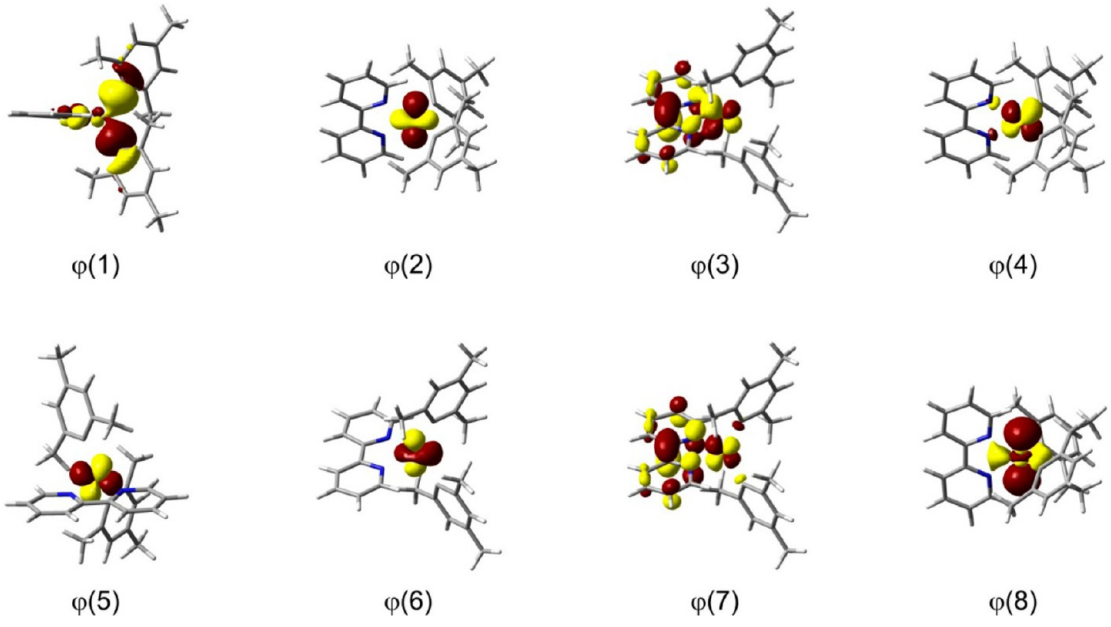

Figure 3. Active orbitals of $[(bpy)Fe^{I}(mes)_2]^-$ (**2**) in the quartet state.

dx.doi.org/10.1021/ct400913z | J. Chem. Theory Comput. XXXX, XXX, XXX−XXX

Table 10. Occupancies of CASSCF Orbitals of $[(bpy)Fe(mes)_2]^-$ (2)

electronic state	1	2	**3**	4	5	6	7	8
Qa	2.00	1.99	**1.20**	1.00	1.00	1.00	**0.80**	0.01
Se	2.00	1.99	**1.00**	1.00	1.00	1.00	**1.00**	0.01

Table 11. NBO Charges (Q) and Löwdin-Spin Densities (ρ) of $[(bpy)Fe^{I}(mes)_2]^-$ (2)

	quartet		sextet	
	Q	ρ	Q	ρ
Fe	1.58	3.46	1.59	3.88
bpy	−0.89	−0.53	−0.90	1.03
mes^1	−0.85	0.03	−0.85	0.04
mes^2	−0.84	0.03	−0.85	0.04

electronic structure corresponds to the neutral bpy coordinated to Fe(0). However, Scarborough and Wieghardt argued against the π-backdonation to bpy and suggested that the electron transfer takes place instead resulting in $[(\eta_6\text{-tol})Fe^{I}(bpy^{\bullet-})]$. Our calculations reveal that the ground state is a closed-shell singlet with one dominant CSF (77% weight, see Supporting Information Tables S3−S5 for details) that is very similar to that in **1**. Here too the bpy is better described as a neutral system and the shortening of the $C_2-C_{2'}$ bond can be ascribed to the extensive π-backbonding originally suggested by Radanovich et al. In this case, when forming the triplet, rather than break the mixing between the metal center and the bpy, the two unpaired electrons reside in metal d orbitals and the bonding and antibonding combinations (φ_4 and φ_7) remain intact; in the triplet state, these two orbitals (φ_4 and φ_7) have occupations of 1.48 and 0.52 electrons. This results in a rather low singlet−triplet energy gap of 9.4 kcal·mol^{-1}. Thus, the system in the triplet state can also be described as Fe(0) and bpy.

For the cobalt complex **4**, the wave function is dominated by a single closed-shell CSF (weight 77%, Supporting Information Tables S7−9). The HOMO is the metal−ligand bonding combination while the LUMO is its antibonding counterpart. Thus, in complex **4** the bpy ligand can be considered a neutral ligand involved in backbonding from the metal center.

In contrast, the vanadium and titanium complexes **5**−**8** are more biradical in nature. They all have wave functions that are dominated by two closed-shell CSFs (see the Supporting Information) with weights of 55−65% and 25−35%. This results in two MOs with occupancies of ∼1. Thus, the ground states of these complexes are better described as open-shell singlets. The wave functions of the very low-lying triplet excitations states have one strongly dominant CSF with one electron is each MO, similar to the overall singlet MO

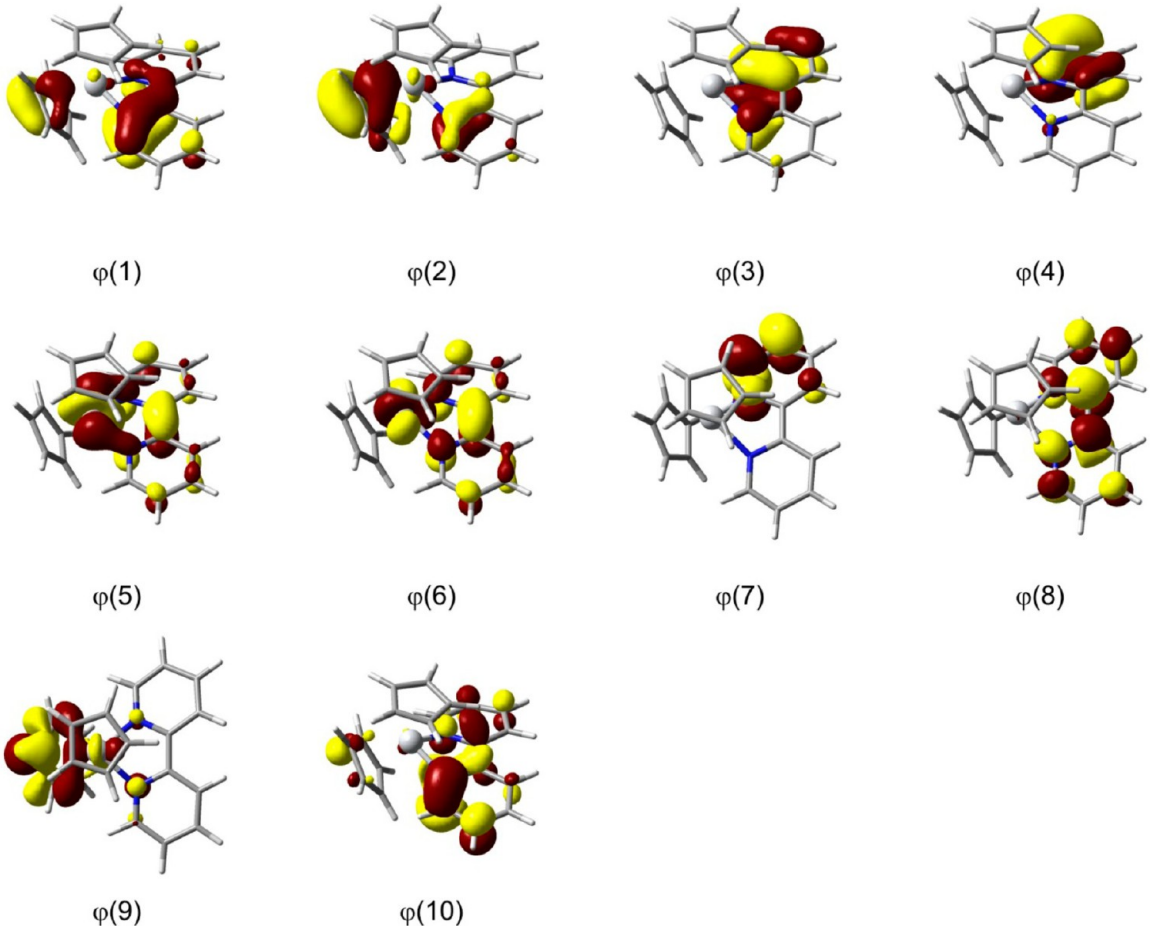

Figure 4. Active orbitals of $[(\eta^5\text{-Cp})_2Ti(bpy)]$ (**6**) in the singlet state.

dx.doi.org/10.1021/ct400913z | J. Chem. Theory Comput. XXXX, XXX, XXX−XXX

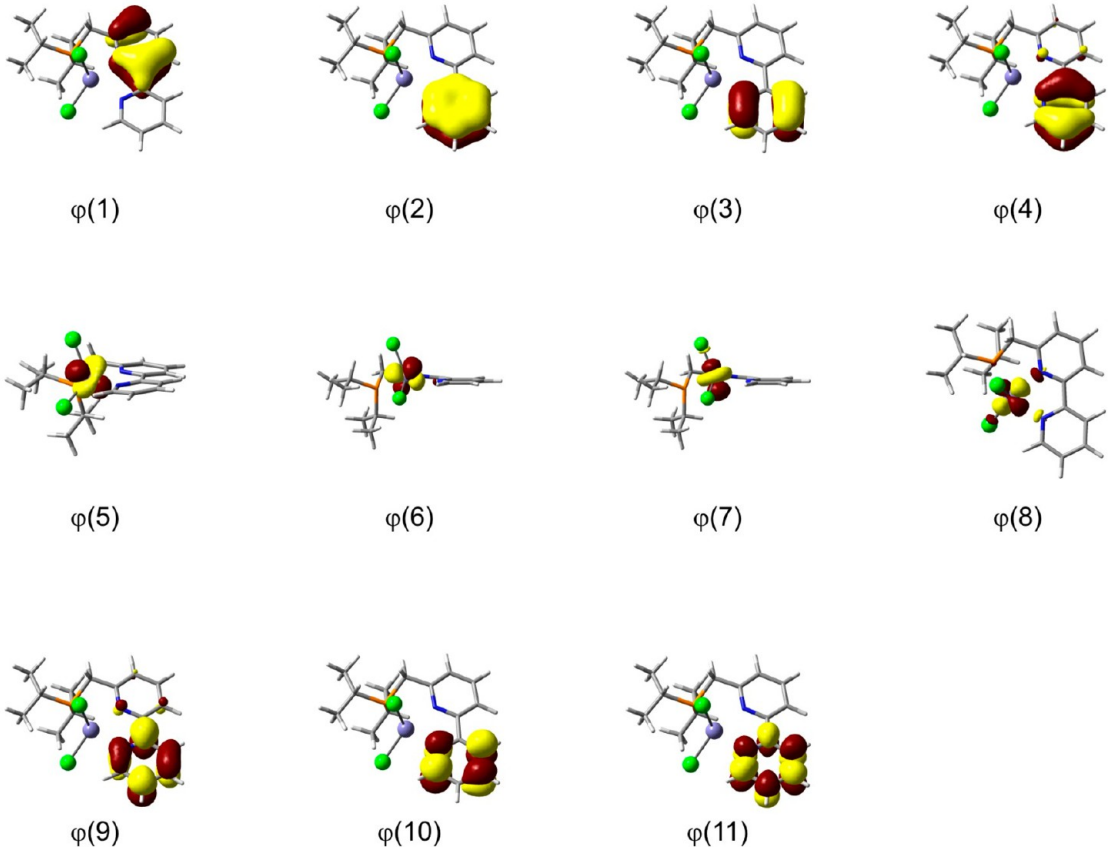

Figure 5. Active orbitals of (^{i}PrCH$_2$bpy)FeCl$_2$ (**9**) in the singlet state.

Table 12. Comparison of Δ*E* (kcal·mol^{-1}) for CASSCF and NEVPT2 with and without the RIJCOSX Approximation

		Δ*E* no RIJCOSX		Δ*E* with RIJCOSX		ΔΔ*E*	
complex	spin state	CASSCF	NEVPT2	CASSCF	NEVPT2	CASSCF	NEVPT2
1a	S[a]	0.0	0.0	0.0	0.0		
	S[b]	−1.9	2.9	−1.8	3.3	−0.1	0.4
	T	8.9	28.1	8.7	28.3	−0.2	0.2
1b	S[a]	0.0	0.0	0.0	0.0		
	S[b]	0.0	3.0	−0.2	2.9	−0.2	−0.1
	T	11.3	28.6	11.2	26.0	−0.1	−2.6
MUE[c]						0.2	0.8

[a]The structure was optimized as a closed-shell singlet at the RM06/SDD(d) level of theory. [b]The structure was optimized as an open-shell singlet at the UM06/SDD(d) level of theory. [c]Mean unsigned error.

occupancies. Since the singlet and triplet states have nearly identical partial atomic charges, and considering the electron density of the triplet state, one can describe the bpy ligand (or bq in the case of **8**) as a radical anion. In the singlet wave function, there is metal−ligand overlap in the key MOs (Table 6, Figure 4 and Figures S15 and S17 in the Supporting Information), akin to the case of **1**. However, considering that there is one electron in a binding combination and one electron is the antibonding combination, this is equivalent to breaking the mixing between these two orbitals. This is what is observed in the MOs of the triplet states (Figures S14, S16 and S18 in the Supporting Information).

Complex **9** has been studied briefly in a previous report by us and we base on discussion there on the calculation done for that report.[6d] It differs from other complexes considered here in that its ground state is a quintet. The CASSCF orbitals, shown in Figure 5, do not indicate any ET or π-backbonding. This is not surprising as the complex has a high-spin electronic state and the occupied MOs do not contain the $C_2-C_{2'}$ π interaction, and thus shortening of $C_2-C_{2'}$ bond in bpy is not observed neither in the X-ray crystallography structure nor in our calculations.[6d]

Past studies have relied on B3LYP, which was used to conclude the presence of an ET state for **2**−**8**. This is in sharp contrast, for complexes **2** and **3**, to the CASSCF and NEVPT2 results obtained here. To be fair, in the past the systems were far too large for tractable CASSCF calculations. However, recent developments, notably the development of the resolution of identity chain of spheres exchange approximation (RIJCOSX)[27] and its application to CASSCF in recent versions of ORCA,[15] have made these, and the associated NEVPT2, calculations feasible, at least for the complexes presented here. As shown in Table 12, for complexes **1a** and **1b**, the mean unsigned errors (MUE) on the excitation energies resulting

dx.doi.org/10.1021/ct400913z | J. Chem. Theory Comput. XXXX, XXX, XXX−XXX

Table 13. Quantitative Comparison (See Text) of the Different Methods Considered[a]

				$\langle S^2 \rangle$ contamination		Qa → Se (2)		D → Qa (5)	
method	type[b]	MUE[c]	MURE[c]	avg	max	ΔE	$\Delta\Delta E$	ΔE	$\Delta\Delta E$
HF	WFT	70.9	53	1.80	4.36	1.6	−2.6	−18.4	−27.5
RI-SCS-MP2	WFT	50.7	304	1.80	4.36	1.2	−3.0	−11.6	−20.7
DSD-BLYP	DH-GGA	18.7	106	0.70	1.95	2.7	−1.5	10.1	+1.0
DSD-PBEP86	DH-GGA	19.4	126	0.71	1.96	2.6	−1.6	−24.3	−33.4
DSD-PBEB95	DH-mGGA	17.8	88	0.68	1.80	2.7	−1.5	25.9	+16.8
PWPB95	DH-mGGA	10.1	43	0.53	1.76	3.3	−0.9	4.8	−4.3
B2PLYP	DH-GGA	23.2	140	0.58	1.79	3.4	−0.8	31.2	22.1
B2GP-PLYP	DH-GGA	23.4	160	1.09	4.06	3.0	−1.2	−45.4	−54.5
B2K-PLYP	DH-GGA	17.9	109	0.70	1.94	2.7	−1.5	11.6	+2.5
B2T-PLYP	DH-GGA	22.3	134	0.64	1.82	3.1	−1.1	−24.3	33.4
M11-L	mGGA	16.1	48	0.22	1.51	5.5	+1.3	5.9	−3.3
MN12-L	mNGA	13.6	62	0.18	0.95	3.2	−1.0	6.1	−3.0
N12	NGA	10.7	19	0.14	1.11	7.4	+3.2	8.3	−0.8
N12-SX	RSH-GGA	15.1	90	0.25	1.31	−6.6	−10.8	5.3	−3.8
B3LYP	GH-GGA	12.2	110	0.27	1.49	−20.1	−24.3	5.4	−3.7
BLYP	GGA	10.2	21	0.15	1.10	7.4	−3.2	8.4	−0.7
BLYP10.41[d]	GH-GGA	8.7	40	0.23	1.31	8.2	+4.0	6.6	−2.5
APDF	GH-GGA	12.6	129	0.35	1.63	−28.4	−32.6	5.0	−4.1
M06	GH-mGGA	8.8	68	0.34	1.14	6.4	+2.2	5.4	−3.7
M06-L	mGGA	6.9	26	0.24	1.35	5.1	+0.9	6.9	−2.1
M11	RSH-mGGA	22.6	240	0.35	1.66	−29.0	−33.2	−17.1	−26.2
MN12-SX	RSH-mGGA	15.3	118	0.26	0.98	−9.9	−14.1	5.2	−3.9
PBE	GGA	9.2	19	0.16	1.19	7.1	+2.9	8.2	−0.9
PBE0	GH-GGA	11.7	95	0.32	1.01	6.4	+2.2	4.9	−4.2
PBE6.37[d]	GH-GGA	8.4	34	0.23	1.35	8.0	3.8	6.8	−2.3
τ-HCTH	mGGA	7.6	22	0.21	1.14	5.4	+1.2	7.0	−2.1
HCTH	GGA	7.8	21	0.21	1.14	5.1	+0.9	7.1	−2.0
τ-HCTHhyb	GH-mGGA	8.9	54	0.27	1.39	5.0	+0.8	5.9	−3.2
B1B95	GH-mGGA	13.4	138	0.30	1.51	−28.9	−33.1	5.2	−3.9
BMK	GA-mGGA	18.8	186	0.29	1.54	−23.8	−28.0	−14.6	−23.7
TPSS	mGGA	10.4	43	0.20	1.36	6.7	+2.5	7.3	−1.8

[a]MUE, ΔE, and $\Delta\Delta E$ are in kcal·mol^{-1}, MURE units are percent, and $\langle S^2 \rangle$ contamination is unitless. [b]WFT = wave function theory, DH = double hybrid, GGA = generalized gradient approximation, mGGA = meta-GGA, NGA = nonseparable gradient approximation, mNGA = meta-NGA, GH = global hybrid, RSH = range-separated hybrid. See ref 31 for details. [c]MUE = mean unsigned error; MURE = mean unsigned relative error (see text). [d]GH-GGA functional with modified percentages of exact Hartree−Fock exchange (see text).

from this RIJCOSX approximation are 0.2 and 0.8 kcal·mol^{-1} for CASSCF and NEVPT2, respectively, and most of the MUE for the latter arises from one high energy species: triplet **1b**.

One detractor from using CASSCF methods is that they are computationally costly and are not straightforward to use; some of the systems studied here were pushing the limits of our available computer resources. Recent years have seen the introduction of a novel class of DFT functionals: the double-hybrids.[45] These functionals include both "exact" Hartree−Fock (HF) exchange and MP2-like (i.e., using Kohn−Sham (KS) rather than HF orbitals) correlation; because of the inclusion of two wave function theory (WFT) based components, the functions are call "double-hybrid" functionals. Because of the inclusion of MP2-like correlation, DFT functionals of this class can have natural orbitals with partial (noninteger) MO occupations. This allows for a wave function much closer to the CASSCF wave function, with some occupation of the σ^* MO, and thus hopefully a more reliable energy prediction. (It should also be noted that double-hybrid functionals are less computationally expensive that CASSCF and are much more "user friendly.")

A number of double hybrid functionals were considered (see Computational Methods for details); RI-SCS-MP2 and Hartree−Fock (HF), the two WFT components of double hybrid functionals, were also included. In addition, we also considered a number of the newer functionals coming out of the Truhlar group: M11-L,[33] MN12-L,[34] N12,[36] and N12-SX;[35] these were chosen based on their leading performance for Truhlar's multireference bond energy (MRBE10)[33] database;[31] a number of other related or more traditional functionals were also considered. In particular, we evaluated, both qualitatively and quantitatively, how well each method compares to the "benchmark" NEVPT2 results.

In Table 13 is the qualitative evaluation of the methods, where we considered both the mean unsigned error (MUE) and mean unsigned relative error (MURE) of each functional, defined as

$$\mathrm{MUE} = \frac{1}{n}\sum_i |\Delta E_{\mathrm{NEVPT2}} - \Delta E_{\mathrm{DFT}}|$$

$$\mathrm{MURE} = \left(\frac{1}{n}\sum_i \frac{|\Delta E_{\mathrm{NEVPT2}} - \Delta E_{\mathrm{DFT}}|}{\Delta E_{\mathrm{NEVPT2}}}\right) \times 100\%$$

We also include six more metrics: average and maximum spin contamination (i.e., deviation of $\langle S^2 \rangle$ from the ideal value of $S(S$

dx.doi.org/10.1021/ct400913z | J. Chem. Theory Comput. XXXX, XXX, XXX−XXX

Table 14. Qualitative Comparison of the Different Methods Used with Incorrect Spin-State Predictions Highlighted in Bold[a]

	complex											
method	**1a**	**1b**	**1c**	**2**	**3**	**4**	**5**	**6**	**7**	**8**	**9**	$n_{correct}$
NEVPT2	S	S	S	Qa	S	S	D	U−S	U−S	U−S	Qi[b]	
CASSCF	S	S	**T**	Qa	S	S	D	U−S	U−S	U−S	Qi[b]	10
HF	**Qi**	**Qi**	**Qi**	Qa	**T**	**T**	**Qa**	U−S	U−S	**T**	Qi	4
RI-SCS-MP2	S	S	S	Qa	S	S	**Qa**	**S**	**S**	**S**	Qi	5
DSD-BLYP	S	S	S	Qa	S	S	D	**S**	**S**	**S**	Qi	8
DSD-PBEP86	S	S	S	Qa	S	S	**Qa**	**S**	**S**	**S**	Qi	7
DSD-PBEB95	S	S	S	Qa	S	S	D	**S**	**S**	**S**	Qi	8
PWPB95	S	S	S	Qa	S	S	D	**S**	**S**	**S**	Qi	8
B2PLYP	S	S	S	Qa	S	S	D	**S**	**S**	**S**	Qi	8
B2GP-PLYP	S	S	S	Qa	S	S	**Qa**	**S**	**S**	**S**	Qi	7
B2K-PLYP	S	S	S	Qa	S	S	D	**S**	**S**	**S**	Qi	8
B2T-PLYP	S	S	S	Qa	S	S	Qa	**S**	**S**	**S**	Qi	7
M11-L	**U−S**	S(0)	S(0)	Qa	**U−S**	**U−S**	D	U−S	U−S	U−S	**U−S**	8
MN12-L	S(0)	S(0)	S(0)	Qa	**U−S**	S(0)	D	U−S	U−S	U−S	**T**	9
N12	S(0)	S(0)	S(0)	Qa	S(0)	S(0)	D	S(0)	U−S	U−S	Qi	10
N12-SX	**U−S**	**U−S**	**U−S**	**Se**	**U−S**	**U−S**	D	U−S	U−S	U−S	**T**	4
B3LYP	**U−S**	**U−S**	**U−S**	**Se**	**U−S**	**U−S**	D	U−S	U−S	U−S	Qi	5
BLYP	S(0)	S(0)	S(0)	Qa	S(0)	S(0)	D	**S(0)**	U−S	U−S	Qi	10
BLYP10.41	S(0)	S(0)	S(0)	Qa	**U−S**	**U−S**	D	U−S	U−S	U−S	Qi	9
APFD	**U−S**	**U−S**	**U−S**	**Se**	**U−S**	**U−S**	D	U−S	U−S	U−S	Qi	5
M06	**U−S**	**U−S**	**U−S**	Qa	**U−S**	**U−S**	D	U−S	U−S	U−S	Qi	6
M06-L	S(0)	S(0)	S(0)	Qa	**U−S**	S(0)	D	U−S	U−S	U−S	Qi	10
M11	**U−S**	**U−S**	**U−S**	**Se**	U−S	U−S	**Qa**	U−S	U−S	U−S	Qi	4
MN12-SX	**U−S**	**U−S**	**U−S**	**Se**	**U−S**	**U−S**	D	U−S	U−S	U−S	Qi	5
PBE	S(0)	S(0)	S(0)	Qa	S(0)	S(0)	D	**S(0)**	U−S	U−S	Qi	10
PBE0	**U−S**	**U−S**	**U−S**	Qa	**U−S**	**U−S**	D	U−S	U−S	U−S	Qi	7
PBE6.37	S(0)	S(0)	S(0)	Qa	**U−S**	U−S	S	U−S	U−S	U−S	Qi	10
τ-HCTH	S(0)	S(0)	S(0)	Qa	S(0)	S(0)	D	U−S	U−S	U−S	Qi	11
HCTH	S(0)	S(0)	S(0)	Qa	S(0)	S(0)	D	U−S	U−S	U−S	Qi	11
τ-HCTHhyb	**U−S**	S(0)	S(0)	Qa	**U−S**	**U−S**	D	U−S	U−S	U−S	Qi	8
B1B95	**U−S**	**U−S**	**U−S**	**Se**	**U−S**	**U−S**	D	U−S	U−S	U−S	Qi	5
BMK	**U−S**	**U−S**	**U−S**	**Se**	**U−S**	**U−S**	**Qa**	U−S	U−S	U−S	Qi	4
TPSS	S(0)	S(0)	S(0)	Qa	**U−S**	S(0)	D	U−S	U−S	U−S	Qi	10

[a] S = singlet, U-S = open-shell (unrestricted) singlet, S(0) = singlet with equal energies for S and U-S (considered as S, see text), D = doublet, T = triplet, Qa = quartet, Qi = quintet, Se = sextet, $n_{correct}$ = number of spin states correctly determined by method. [b] Taken from the RIJK-NEVPT2/TZVP results from ref 6d.

+ 1)) for all complexes studied, the Qa → Se excitation energy and error for **2**, and the D → Qa excitation energy and error for **5**. Also noted are the types of method considered. In Table 14 we compare the predicted ground state of all methods. The raw data with all transition energies is provided in the Supporting Information (see Tables S27−S55).

Reviewing this data, certain observations are apparent. The double hybrid functionals do not predict a situation where the open-shell singlet is favored over the closed-shell. Thus, while complexes **1a−c** and **3** are always correctly predicted as closed-shell systems, so too are complexes **6−8**, even though NEVPT2 predicts them to be open-shell singlets. This reflects the behavior of RI-SCS-MP2. On the other hand, hybrid functions tend to favor open-shell systems and therefore correctly predict the spin states of complexes **6−8** but not complexes **1a−c** and **3**. Even though they are the oldest class of functionals, the GGA functionals (BLYP, PBE, HCTH) and meta-GGA functionals (M06-L, τ-HCTH, TPSS) appear to perform best, as does the newer NGA functional N12. On the basis of both the qualitative and quantitative factors, τ-HCTH and HCTH are the best performers: both are the only two methods to correctly predict all eleven spin-states and they (consequently) have the second-lowest MUEs. M06-L has the lowest MUE but the open-shell singlet for **3** is 0.9 kcal·mol^{-1} lower in energy than the closed-shell singlet. If one considers MURE, which may be a better measure as we are comparing excitation energies of different magnitudes, then all these nonhybrid functionals have similar performances.

While τ-HCTH and HCTH are the best performers correctly predicting all eleven spin states, if these functionals are unavailable in a given electronic structure code there are a few alternate functionals that also performed well. There are six functionals that correctly predicted ten of the spin states correctly (Table 15). Four of these functionals predict that complex **6** is a closed-shell singlet instead of an open-shell singlet (i.e., the unrestricted energy calculation gave the same energy as the restricted calculation). M06-L and TPSS predict that complex **3** is open-shell while NEVPT2 predicts a closed-shell system. However, the energy differences between the open-shell and closed-shell singlets are so small (<1 kcal·mol^{-1}) that this gap is not overly meaningful.

Another consequence of the hybrid functionals favoring high spin systems, such as the open-shell singlet over the closed-shell singlet, is that they also favor the sextet spin-state for **2** rather

Table 15. The "10-out-of-11" DFT Functionals and Their Problematic Complexes

DFT functional	problematic system	predicted spin state		
		DFT	NEVPT2	ΔE (S → U-S)
N12	**6**	S(0)	U-S	
BLYP	**6**	S(0)	U-S	
M06-L	**3**	U-S	S	−0.93 kcal·mol^{-1}
PBE	**6**	S(0)	U-S	
TPSS	**3**	U-S	S	−0.05 kcal·mol^{-1}

than the quartet. Three hybrids do correctly predict the quartet: PBE0, M06, and τ-HCTHhyb. It might be postulated that the latter two do so because of the kinetic energy density (τ) included in their functional form. It has been observed that τ can help alleviate other problems arising from large fractions of HF in the functional form—such as in the performance of "kinetics" functions like BMK.[42] One could counter with the poor performances of the hybrid meta-GGA functionals B1B95 and BMK. However, whereas τ-HCTHhyb has τ in its exchange functional and M06 includes it in both the exchange and correlation functionals, B1B95 only has τ in its correlation functionals (i.e., B95, and then only as a simple multiplicative factor in the same-spin term that ensures a single electron will have no (spurious) self-correlation energy). It would appear that the negative effects of including Hartree−Fock exchange in the functional form can be counterbalanced by including τ in the exchange functional. BMK, which is essentially a reparameterized τ-HCTHhyb for main-group kinetics, apparently has too much HF exchange to be balanced out by τ and thus its poor performance. A related assessment is the D → Qa excitation in **5**, where the D state is the ground state. However, this is less of a torture test and most functionals do reasonably well. At this point, we do not have an explanation as to why PBE0 alone of all the nonmeta-GGA functionals correctly predicts the quartet ground state for **2**.

One particularly challenging case for DFT functionals in the high-spin complex **9**. While most of the functionals tested manage to correctly predict the quintet state, many severely underestimate the quintet-triplet and quintet-singlet transition energies (see Supporting Information Tables S27−S55). This is most pronounced for GGA and mGGA functionals but less so for the hybrid and double hybrid functionals. Thus, while most functionals will likely correctly predict the ground state of such high-spin complexes, care should be exercised when considering the relative energies of the excited states (other spin states).

From the spin contaminations (Table 13 and Supporting Informatin Tables S27−S55), one observes that there is significant contamination, especially in the lower spin states, from higher spin states. The deviations are in general larger for the double-hybrid functionals (average deviations are in the range of 0.58−1.80) than for the hybrid and GGA functionals (average deviations in the range of 0.14−0.35); the functionals that better predict spin-states are at the bottom of this range. This is a clear indicator that many of the functionals have problems correctly describing the spin-states of many of these systems. Similar observations on UHF/UKS instabilities have been made for the W4-11 test set.[63]

If one were to consider the theory behind DFT, this preference for an open-shell singlet can be understood. DFT, excluding the double hybrid functionals, is an approximately variational method (were the exact exchange-correlation functional known, then the method would truly be variational) and thus any change to the wave function that lowers the energy is a better approximation to the ground state wave function and energy. By moving from the RKS to the UKS formulation, one relaxes the constraints on the orbitals during the SCF optimization, giving a more flexible system and as a consequence lowering the energy. Thus, one can always expect the UKS energy to be less than or equal to the RKS energy (i.e., $E_{UKS} \leq E_{RKS}$); a similar observation was made for Fe_2, Fe_2^- and FeO^+ when symmetry constraints on the orbitals were eased.[64] However, this energy lowering is, as noted from the comparison to the NEVPT2 results, an artifact of the method's inability to properly describe the wave function. For a number of the systems in Table 14, the open-shell and closed-shell singlets have equal energies (indicated in the table as "S(0)"); this is a common observation for systems that are well-behaved.

The above argument does not hold for the double hybrid functionals. Because they include an MP2-like component, which itself is nonvariational, these functionals are nonvariational. Thus, it cannot be expected a priori that easing the constraints would lower the energy. In fact, none of these functionals predict an open-shell singlet in any case, even those where such a situation is predicted by NEVPT2 (i.e., for complexes **6**−**8**). This reflects the same inability of MP2. It may not be surprising that these functionals perform so poorly for these properties as these functionals were primarily designed to improve the description of dynamic correlation and especially dispersion forces, rather than the static (nondynamic) correlation that affects the calculations on these systems.

In Figures 6 and 7 and S19−S21 in the Supporting Information, we compare that key MOs of various complexes optimized with different methods. Generally, the CASSCF calculations show mixing of a d-orbital of a transition metal with the antibonding orbital of the bpy moiety in the ground state forming a new bonding molecular orbital and its antibonding partner. In the restricted formalism (i.e., RKS), DFT based methods, particularly B3LYP, DSD-PBEP86, and M06, also predict this same mixing. However, such wave functions are found to be unstable. This instability arises from a fact that CASSCF predicts that the LUMO of these complexes are partially occupied. This is a situation that cannot be treated by single-configuration methods, including DFT. Using the unrestricted formalism (i.e., UKS) leads to stable wave functions, but the mixing of the d-orbital and the bpy LUMO almost vanishes, causing the false prediction of species with biradical character. Two of the functionals tested (N12 and τ-HCTH) do mix these orbitals to form a pair of bonding and antibonding molecular orbitals (Figures 6 and 7). Nonetheless, there are still some issues with these functionals. While they do predict the orbital mixing, because by construct DFT requires integer orbital occupancies they do not allow the partial occupation of the LUMO as observed in CASSCF. Moreover, these functionals seem to always predict this mixing, even in cases like triplet cases of **6** and **8** (Figures 6cd and 7cd) where CASSCF predicts no mixing.

One trick that has been used in the past to improve the performance of DFT functionals for transition metals is to reduce the percentage of "exact" Hartree−Fock exchange incorporated into the hybrid functional.[65] We reduced the amount of exact exchange in B3LYP and PBE0 to 5%, 10%, and 15%. We then plotted the MUE of the functionals, along with the standard hybrid (i.e., 20% and 25% exact exchange,

dx.doi.org/10.1021/ct400913z | J. Chem. Theory Comput. XXXX, XXX, XXX−XXX

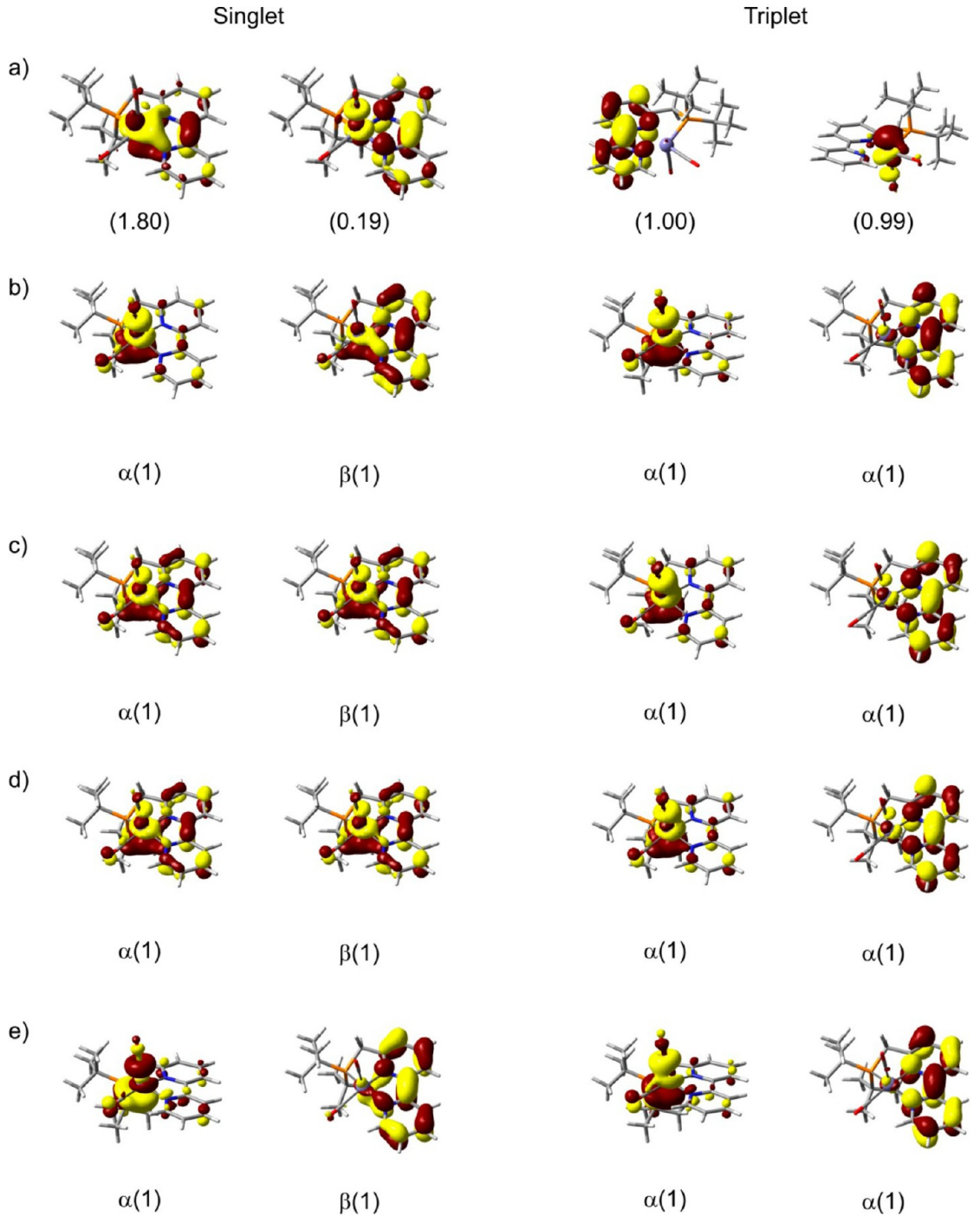

Figure 6. Comparison of selected orbitals of [(^{t}Bu$_2$PCH$_2$bpy)Fe(CO)$_2$] (**1a**) optimized at different levels of theory: (a) CASSCF, (b) B3LYP, (c) τ-HCTH (d) N12, and (e) PWPB95. The occupation numbers of each orbital are in brackets.

respectively) and GGA (i.e., 0% exact exchange) functionals, versus the amount of exact exchange and fitted the results to a third-order polynomial (Figure 8, raw data is provided in the Supporting Information in Tables S56−S63). Minima were found at 10.41% and 6.37% for B3LYP and PBE0, respectively. The MUEs and spin-states were recalculated with these levels of exact exchange. (These new functionals are denoted as BLYP10.41 and PBE6.37.) These new functionals give a slight improvements in MUE over their GGA analogues, and more so over the standard hybrid functionals (Table 13). Nonetheless, if one considers the performance vis-à-vis spin-state predictive ability, neither new functional outperforms its GGA counterpart, and BLYP10.41 does even worse (Table 14). Furthermore, neither new functional outperforms τ-HCTH or HCTH, either in MUE or spin-state predictions.

One of the key issues with the systems studied here is static (nondynamical) correlation. Recently, Becke and co-workers published a new functional ("Becke13" or $E_{\mathrm{XstrongC}}^{\mathrm{B13}}$) specifically designed for static correlation,[66] which would seem very appropriate for this study. Unfortunately, this functional is not available in any distributed electronic structure code and is likely too computationally expensive for the systems studied here.[67] Nonetheless, it would be interesting to follow this functional as its development progresses.

dx.doi.org/10.1021/ct400913z | J. Chem. Theory Comput. XXXX, XXX, XXX−XXX

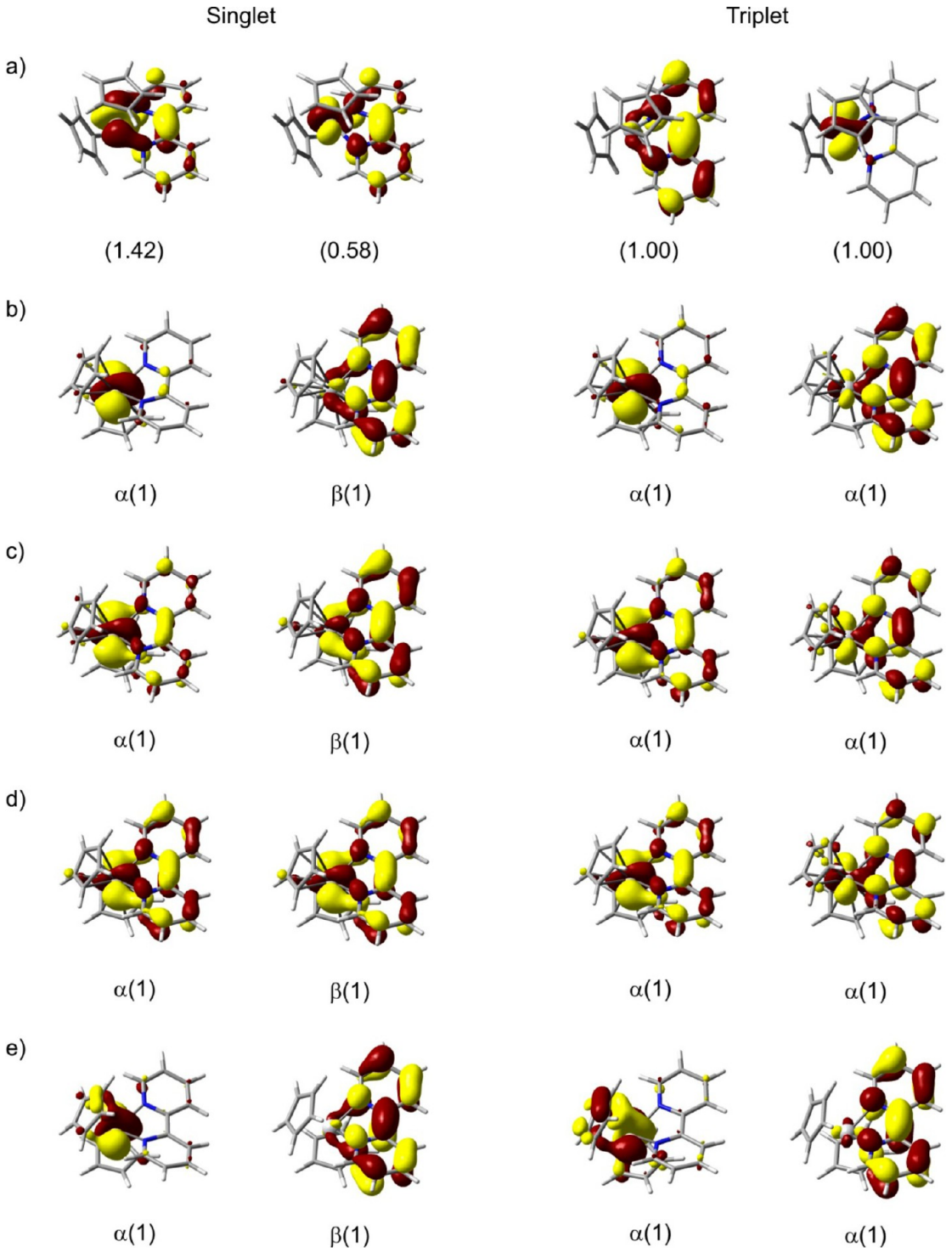

Figure 7. Comparison of selected orbitals of (bpy)Ti(Cp)$_2$ (**6**) optimized at different levels of theory: (a) CASSCF, (b) B3LYP, (c) τ-HCTH, (d) N12, and (e) PWPB95. The occupation numbers of each orbital are in brackets.

CONCLUSIONS

A series of first-row transition metal complexes of bipyridine were examined. There are two competing phenomena that can occur. In certain complexes, such as $(R_2CH_2bpy)Fe(CO)_2$ (**1a**−**c**) and (bpy)Fe(η^6-tol) (**3**), π-backbonding from an occupied metal d-orbital to the ligand LUMO occurs; it is this bonding interaction that results in the observed C_2−$C_{2'}$ bond shortening. In other complexes, such as in the vanadium and titanium complexes **5**−**8**, electron transfer (ET) takes place and the bpy ligand does indeed behave as a radical anion (i.e., as bpy$^{\bullet-}$). It is often hard to say in advance which scenario is more likely, especially in the absence of any experimental indicators. The C_2−$C_{2'}$ bond has in the past been used as an experimental indicator for the formation of a bpy radical anion, however this bond was found here to be sensitive to both processes. Therefore, multireference calculations are needed to distinguish between these two processes.

dx.doi.org/10.1021/ct400913z | J. Chem. Theory Comput. XXXX, XXX, XXX−XXX

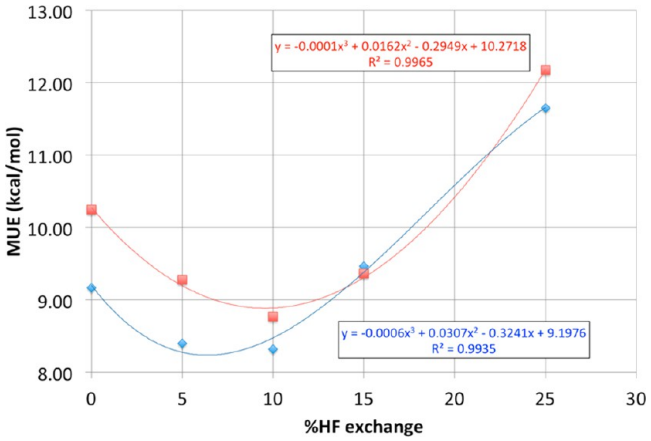

Figure 8. Plot of MUE (kcal·mol^{-1}) versus percentage of "exact" Hartree−Fock exchange in B3LYP (red) and PBE0 (blue).

On the basis of our multireference benchmark calculations, a variety of more amenable methods were evaluated. Hybrid DFT functionals, notably B3LYP, have been widely used in the past to evaluate the electronic structure of these complexes. This functional, however, was shown here to provide erroneous conclusions: several of the closed-shell systems were instead predicted to be open-shell. The more advanced double hybrid functionals also failed to consistently provide the correct answer but in this case failed for the open-shell systems, which they predicted to be closed-shell. In principle, one should run CASSCF and NEVPT2 calculations in order to accurately determine the nature of these complexes. Nonetheless, despite many recent advances, these calculations are very expensive, not user-friendly, and may exceed for larger complexes one's typically available resources. Because of this, a number of different functionals were evaluated, and it was found that τ-HCTH and HCTH had the lowest errors and correctly predicted the electronic states of all eleven test cases; M06-L, N12, BLYP, PBE, and TPSS also fared well correctly predicting ten of the states. Thus, these functionals are likely suitable for those cases where CASSCF is too costly, although care should still be taken to make sure that the obtained results are reasonable.

■ ASSOCIATED CONTENT

Supporting Information

Additional tables of data and figures, and optimized Cartesian (*XYZ*) coordinates of complexes **1a**−**c**. This material is available free of charge via the Internet at http://pubs.acs.org.

■ AUTHOR INFORMATION

Corresponding Author

*E-mail: mark.a.iron@weizmann.ac.il.

Notes

The authors declare no competing financial interest.

■ ACKNOWLEDGMENTS

P.M. acknowledges the Feinberg Graduate School of the Weizmann Institute of Science for a postdoctoral fellowship.

■ DEDICATION

This paper is dedicated to the memories of Dr. habil. Detlef Schröder and Prof. Michael Bendikov who passed away before their time.

■ REFERENCES

(1) For recent reviews, see (a) Milstein, D. *Top. Catal.* **2010**, *53*, 915−923. (b) Gunanathan, C.; Milstein, D. *Top. Organomet. Chem.* **2011**, *37*, 55−84. (c) Gunanathan, C.; Milstein, D. *Acc. Chem. Res.* **2011**, *44*, 588−602. (d) Gunanathan, C.; Milstein, D. *Science* **2013**, *341*, 1229712. See also: (e) Michos, D.; Luo, X.-L.; Crabtree, R. H. *J. Chem. Soc., Dalton Trans.* **1992**, 1735−1738. (f) Marchi, A.; Marvelli, L.; Rossi, R.; Magon, L.; Uccelli, L.; Bertolasi, V.; Ferretti, V.; Zanobini, F. *J. Chem. Soc., Dalton Trans.* **1993**, 1281−1286. (g) Zhang, J.; Leitus, G.; Ben-David, Y.; Milstein, D. *J. Am. Chem. Soc.* **2005**, *127*, 10840−10841. (h) Zhang, J.; Leitus, G.; Ben-David, Y.; Milstein, D. *Angew. Chem., Int. Ed.* **2006**, *45*, 1113−1115. (i) Gunanathan, C.; Ben-David, Y.; Milstein, D. *Science* **2007**, *317*, 790−792. (j) Ozerov, O. V.; Watson, L. A.; Pink, M.; Caulton, K. G. *J. Am. Chem. Soc.* **2007**, *129*, 6003−6016. (k) Gunanathan, C.; Milstein, D. *Angew. Chem., Int. Ed.* **2008**, *47*, 8661−8664. (l) Friedrich, A.; Schneider, S. *ChemCatChem* **2009**, *1*, 72−73. (m) Tanaka, R.; Yamashita, M.; Nozaki, K. *J. Am. Chem. Soc.* **2009**, *131*, 14168−14169. (n) Balaraman, E.; Gnanaprakasam, B.; Shimon, L. J. W.; Milstein, D. *J. Am. Chem. Soc.* **2010**, *132*, 16756−16758. (o) Gnanaprakasam, B.; Zhang, J.; Milstein, D. *Angew. Chem., Int. Ed.* **2010**, *49*, 1468−1471. (p) Gunanathan, C.; Gnanaprakasam, B.; Iron, M. A.; Shimon, L. J. W.; Milstein, D. *J. Am. Chem. Soc.* **2010**, *132*, 14763−14795. (q) Balaraman, E.; Ben-David, Y.; Milstein, D. *Angew. Chem., Int. Ed.* **2011**, *50*, 11702−11705. (r) Balaraman, E.; Gunanathan, C.; Zhang, J.; Shimon, L. J. W.; Milstein, D. *Nature Chem.* **2011**, *3*, 609−614. (s) Gnanaprakasam, B.; Balaraman, E.; Ben-David, Y.; Milstein, D. *Angew. Chem., Int. Ed.* **2011**, *50*, 12240−12244. (t) Huff, C. A.; Sanford, M. S. *J. Am. Chem. Soc.* **2011**, *133*, 18122−18125. (u) Langer, R.; Diskin-Posner, Y.; Leitus, G.; Shimon, L. J. W.; Ben-David, Y.; Milstein, D. *Angew. Chem., Int. Ed.* **2011**, *50*, 9948−9952. (v) Tanaka, R.; Yamashita, M.; Chung, L. W.; Morokuma, K.; Nozaki, K. *Organometallics* **2011**, *30*, 6742−6750. (w) Zeng, H.; Guan, Z. *J. Am. Chem. Soc.* **2011**, *133*, 1159−1161. (x) Balaraman, E.; Fogler, E.; Milstein, D. *Chem. Commun.* **2012**, *48*, 1111−1113. (y) Hunsicker, D. M.; Dauphinais, B. C.; McIlrath, S. P.; Robertson, N. J. *Macromol. Rapid Commun.* **2012**, *33*, 232−236. (z) Srimani, D.; Balaraman, E.; Gnanaprakasam, B.; Ben-David, Y.; Milstein, D. *Adv. Synth. Catal.* **2012**, *354*, 2403−2406. (aa) Balaraman, E.; Khaskin, E.; Leitus, G.; Milstein, D. *Nature Chem.* **2013**, *5*, 122−125. (ab) Michlik, S.; Kempe, R. *Nature Chem.* **2013**, *5*, 140−144. (ac) Srimani, D.; Ben-David, Y.; Milstein, D. *Angew. Chem., Int. Ed.* **2013**, *52*, 4012−4015. (ad) Zell, T.; Butschke, B.; Ben-David, Y.; Milstein, D. *Chem.—Eur. J.* **2013**, *19*, 8068−8072.

(2) (a) Vogt, M.; Gargir, M.; Iron, M. A.; Diskin-Posner, Y.; Ben-David, Y.; Milstein, D. *Chem.—Eur. J.* **2012**, *18*, 9194−9197. (b) Huff, C. A.; Kampf, J. W.; Sanford, M. S. *Organometallics* **2012**, *31*, 4643−4645. (c) Vogt, M.; Rivada-Wheelaghan, O.; Iron, M. A.; Leitus, G.; Diskin-Posner, Y.; Shimon, L. J. W.; Ben-David, Y.; Milstein, D. *Organometallics* **2013**, *32*, 300−308.

(3) Montag, M.; Zhang, J.; Milstein, D. *J. Am. Chem. Soc.* **2012**, *134*, 10325−10328.

(4) Huff, C. A.; Kampf, J. W.; Sanford, M. S. *Chem. Commun.* **2013**, *49*, 7147−7149.

(5) Vogt, M.; Nerush, A.; Iron, M. A.; Leitus, G.; Diskin-Posner, Y.; Shimon, L. J. W.; Ben-David, Y.; Milstein, D. *J. Am. Chem. Soc.* **2013**, *135*, 17004−17018.

(6) (a) Zhang, J.; Gandelman, M.; Herrman, D.; Leitus, G.; Shimon, L. J. W.; Ben-David, Y.; Milstein, D. *Inorg. Chim. Acta* **2006**, *359*, 1955−1960. (b) Langer, R.; Leitus, G.; Ben-David, Y.; Milstein, D. *Angew. Chem., Int. Ed.* **2011**, *50*, 2120−2124. (c) Langer, R.; Iron, M. A.; Konstantinovski, L.; Diskin-Posner, Y.; Leitus, G.; Ben-David, Y.; Milstein, D. *Chem.—Eur. J.* **2012**, *18*, 7196−7209. (d) Zell, T.; Langer, R.; Iron, M. A.; Konstantinovski, L.; Shimon, L. J. W.; Diskin-Posner, Y.; Leitus, G.; Balaraman, E.; Ben-David, Y.; Milstein, D. *Inorg. Chem.* **2013**, *52*, 9636−9649 Note that in this paper it was stated that CASSCF(10,8) and RIJCOSX were used; however, further review while preparing this paper showed that for the (^{i}Pr$_2$PCH$_2$pby)FeCl$_2$ complex (**9**), the actual active space was (12,11) and that in all cases RIJK was used instead of RIJCOSX. It is not expected that the use of

either RIJCOSX or RIJK would have any significant impact on the results. (e) Zell, T.; Milko, P.; Fillman, K. L.; Diskin-Posner, Y.; Bendikov, T.; Iron, M. A.; Leitus, G.; Ben-David, Y.; Neidig, M. L.; Milstein, D., submitted for publication.
(7) Khaskin, E.; Diskin-Posner, Y.; Weiner, L.; Leitus, G.; Milstein, D. *Chem. Commun.* **2013**, *49*, 2771−2773.
(8) Irwin, M.; Jenkins, R. K.; Denning, M. S.; Krämer, T.; Grandjean, F.; Long, G. J.; Herchel, R.; McGrady, J. E.; Goicoechea, J. M. *Inorg. Chem.* **2010**, *49*, 6160−6171.
(9) Scarborough, C. C.; Wieghardt, K. *Inorg. Chem.* **2011**, *50*, 9773−9793.
(10) Radanovich, L. J.; Eyring, M. W.; Groshens, T. J.; Klabunde, K. J. *J. Am. Chem. Soc.* **1982**, *104*, 2816−2819.
(11) (a) Bowman, A. C.; Sproules, S.; Wieghardt, K. *Inorg. Chem.* **2012**, *51*, 3707−3717. (b) Scarborough, C. C.; Sproules, S.; Doonan, C. J.; Hagen, K. S.; Weyhermüller, T.; Wieghardt, K. *Inorg. Chem.* **2012**, *51*, 699−6982. (c) Bowman, A. C.; England, J.; Sproules, S.; Weyhermüller, T.; Wieghardt, K. *Inorg. Chem.* **2013**, *52*, 2242−2256. (d) Wang, M.; England, J.; Weyhermüller, T.; Kokatam, S.-L.; Pollock, C. J.; DeBeer, S.; Shen, J.; Yap, G. P. A.; Theopold, K. H.; Wieghardt, K. *Inorg. Chem.* **2013**, *52*, 4472−4487. (e) England, J.; Wieghardt, K. *Inorg. Chem.* **2013**, *52*, 10067−10079.
(12) Zhang, I. Y.; Xu, X. *Int. Rev. Phys. Chem.* **2011**, *30*, 115−160.
(13) (a) Zheng, J.; Zhao, Y.; Truhlar, D. G. *J. Chem. Theory Comput.* **2009**, *5*, 808−821. (b) Karton, A.; Gruzman, D.; Martin, J. M. L. *J. Phys. Chem. A* **2009**, *113*, 8434−8447. (c) Gruzman, D.; Karton, A.; Martin, J. M. L. *J. Phys. Chem. A* **2009**, *113*, 11974−11983. (d) Goerigk, L.; Grimme, S. *J. Chem. Theory Comput.* **2011**, *7*, 3272−3277. (e) Grimme, S.; Mück-Lichtenfeld, C. *Isr. J. Chem.* **2012**, *52*, 180−192. (f) Martin, J. M. L. *J. Phys. Chem. A* **2013**, *117*, 3118−3132.
(14) Frisch, M. J.; Trucks, G. W.; Schlegel, H. B.; Scuseria, G. E.; Robb, M. A.; Cheeseman, J. R.; Scalmani, G.; Barone, V.; Mennucci, B.; Petersson, G. A.; Nakatsuji, H.; Caricato, M.; Li, X.; Hratchian, H. P.; Izmaylov, A. F.; Bloino, J.; Zheng, G.; Sonnenberg, J. L.; Hada, M.; Ehara, M.; Toyota, K.; Fukuda, R.; Hasegawa, J.; Ishida, M.; Nakajima, T.; Honda, Y.; Kitao, O.; Nakai, H.; Vreven, T.; Montgomery, J. A., Jr.; Peralta, J. E.; Ogliaro, F.; Bearpark, M.; Heyd, J. J.; Brothers, E.; Kudin, K. N.; Staroverov, V. N.; Keith, T.; Kobayashi, R.; Normand, J.; Raghavachari, K.; Rendell, A.; Burant, J. C.; Iyengar, S. S.; Tomasi, J.; Cossi, M.; Rega, N.; Millam, J. M.; Klene, M.; Knox, J. E.; Cross, J. B.; Bakken, V.; Adamo, C.; Jaramillo, J.; Gomperts, R.; Stratmann, R. E.; Yazyev, O.; Austin, A. J.; Cammi, R.; Pomelli, C.; Ochterski, J. W.; Martin, R. L.; Morokuma, K.; Zakrzewski, V. G.; Voth, G. A.; Salvador, P.; Dannenberg, J. J.; Dapprich, S.; Daniels, A. D.; Farkas, O.; Foresman, J. B.; Ortiz, J. V.; Cioslowski, J.; Fox, D. J. *Gaussian 09*, Revision D.01; Gaussian, Inc.: Wallingford, CT, 2013.
(15) Neese, F. *WIREs Comput. Mol. Sci.* **2012**, *2*, 73−78.
(16) Neese, F.; Wennmohs, F.; Becker, U.; Bykov, D.; Ganyushin, D.; Hansen, A.; Izsak, R.; Liakos, D. G.; Kollmar, C.; Kossmann, S.; Pantazis, D. A; Petrenko, T.; Reimann, C.; Riplinger, C.; Roemelt, M.; Sandhöfer, B.; Schapiro, I.; Sivalingam, K.; Wezisla, B.; Kállay, M.; Grimme, S.; Valeev, E. *Orca, an ab initio, DFT and semiempirical SCF-MO package*, Version 2.9.0; Max Planck Institute for Bioinorganic Chemistry, Mülheim an der Ruhr, Germany, 2012.
(17) Stevens, P. J.; Devlin, F. J.; Chabalowski, C. F.; Frisch, M. J. *J. Phys. Chem.* **1994**, *98*, 11623−11627.
(18) Zhao, Y.; Truhlar, D. G. *Theor. Chem. Acc.* **2008**, *120*, 215−241.
(19) Becke, A. D. *J. Chem. Phys.* **1993**, *98*, 5648−5652.
(20) Becke, A. D. *Phys. Rev. A* **1988**, *38*, 3098−3100.
(21) Lee, C.; Yang, W.; Parr, R. G. *Phys. Rev. B* **1988**, *38*, 785−789.
(22) Zhao, Y.; Truhlar, D. G. *Acc. Chem. Res.* **2008**, *41*, 157−167.
(23) (a) Hegarty, D.; Robb, M. A. *Mol. Phys.* **1979**, *38*, 1795−1812. (b) Eade, R. H. A.; Robb, M. A. *Chem. Phys. Lett.* **1981**, *83*, 362−368. (c) Schlegel, H. B.; Robb, M. A. *Chem. Phys. Lett.* **1982**, *93*, 43−46. (d) Bernardi, F.; Andrea, B.; McDouall, J. J. W.; Robb, M. A.; Schlegel, H. B. *Fareaday Symp. Chem. Soc.* **1984**, *19*, 137−147. (e) Frisch, M. J.; Ragazos, I. N.; Robb, M. A.; Schlegel, H. B. *Chem. Phys. Lett.* **1992**, *189*, 524−528. (f) Yamamoto, N.; Vreven, T.; Robb, M. A.; Frisch, M. J.; Schlegel, H. B. *Chem. Phys. Lett.* **1996**, *250*, 373−378. (g) Schmidt, M. W.; Gordon, M. S. *Annu. Rev. Phys. Chem.* **1998**, *49*, 233−266.
(24) (a) Angeli, C.; Cimiraglia, R.; Evangelisti, S.; Leininger, T.; Malrieu, J.-P. *J. Chem. Phys.* **2001**, *114*, 10252−10264. (b) Angeli, C.; Cimiraglia, R.; Malrieu, J.-P. *Chem. Phys. Lett.* **2001**, *350*, 297−305. (c) Angeli, C.; Cimiraglia, R.; Malrieu, J.-P. *J. Chem. Phys.* **2002**, *117*, 9138−9153.
(25) Dolg, M. In *Modern Methods and Algorithms of Quantum Chemistry*; Grotendorst, J., Ed. John von Neumann Institute for Computing: Jülich, 2000; Vol. *1*, pp 479−508.
(26) Dunning, T. H., Jr.; Hay, P. J. In *Modern Theoretical Chemistry 3. Methods of Electronic Structure Theory*; Schaefer, H. F., III, Ed. Plenum Press: New York, 1976; Vol. *3*, pp 1−28.
(27) (a) Neese, F. *J. Comput. Chem.* **2003**, *24*, 1740−1747. (b) Neese, F.; Wennmohs, F.; Hansen, A.; Becker, U. *Chem. Phys.* **2009**, *356*, 98−109. (c) Kossmann, S.; Neese, F. *Chem. Phys. Lett.* **2009**, *481*, 240−243. (d) Kossmann, S.; Neese, F. *J. Chem. Theory Comput.* **2010**, *6*, 2325−2338. (e) Izsák, R.; Neese, F. *J. Chem. Phys.* **2011**, *135*, 144105.
(28) (a) Schäfer, A.; Horn, H.; Ahlrichs, R. *J. Chem. Phys.* **1992**, *97*, 2571−2577. (b) Weigend, F.; Ahlrichs, R. *Phys. Chem. Chem. Phys.* **2005**, *7*, 3297−3305.
(29) (a) Andrae, D.; Häußermann, U.; Dolg, M.; Stoll, H.; Preuß, H. *Theor. Chim. Acta* **1990**, *77*, 123−141. (b) Kaupp, M.; Schleyer, P. v. R.; Stoll, H.; Preuss, H. *J. Chem. Phys.* **1991**, *94*, 1360−1366. (c) Leininger, T.; Nicklass, A.; Küchle, W.; Stoll, H.; Dolg, M.; Bergner, A. *Chem. Phys. Lett.* **1996**, *255*, 274−280. (d) Metz, B.; Stoll, H.; Dolg, M. *J. Chem. Phys.* **2000**, *113*, 2563−2569. (e) Peterson, K. A.; Figgen, D.; Goll, E.; Stoll, H.; Dolg, M. *J. Chem. Phys.* **2003**, *119*, 11113−11123.
(30) (a) Feller, D. *J. Comput. Chem.* **1996**, *17*, 1571−1586. (b) Schuchardt, K. L.; Didier, B. T.; Elsethagen, T.; Sun, L.; Gurumoorthi, V.; Chase, J.; Li, J.; Windus, T. L. *J. Chem. Inf. Model.* **2007**, *47*, 1045−1052.
(31) Peverati, R.; Truhlar, D. G. *arXiv.org* 2013, *physics.chem-ph*, 1212.0944v2 (accessed Oct 21, 2013).
(32) Peverati, R.; Truhlar, D. G. *J. Phys. Chem. Lett.* **2011**, *2*, 2810−2817.
(33) Peverati, R.; Truhlar, D. G. *J. Phys. Chem. Lett.* **2012**, *3*, 117−124.
(34) Peverati, R.; Truhlar, D. G. *Phys. Chem. Chem. Phys.* **2012**, *14*, 13171−13174.
(35) Peverati, R.; Truhlar, D. G. *Phys. Chem. Chem. Phys.* **2012**, *14*, 16187−16191.
(36) Peverati, R.; Truhlar, D. G. *J. Chem. Theory Comput.* **2012**, *8*, 2310−2319.
(37) (a) Perdew, J. P.; Burke, K.; Ernzerhof, M. *Phys. Rev. Lett.* **1996**, *77*, 3865−3868. (b) Perdew, J. P.; Burke, K.; Ernzerhof, M. *Phys. Rev. Lett.* **1997**, *78*, 1396.
(38) Adamo, C.; Barone, V. *J. Chem. Phys.* **1999**, *110*, 6158−6170.
(39) Zhao, Y.; Truhlar, D. G. *J. Chem. Phys.* **2006**, *125*, 194101.
(40) (a) Hamprecht, F. A.; Cohen, A. J.; Tozer, D. J.; Handy, N. C. *J. Chem. Phys.* **1998**, *109*, 6264−6271. (b) Boese, A. D.; Doltsinis, N. L.; Handy, N. C.; Sprik, M. *J. Chem. Phys.* **2000**, *112*, 1670−1678. (c) Boese, A. D.; Handy, N. C. *J. Chem. Phys.* **2001**, *114*, 5497−5503.
(41) Boese, A. D.; Handy, N. C. *J. Chem. Phys.* **2002**, *116*, 9559−9569.
(42) Boese, A. D.; Martin, J. M. L. *J. Chem. Phys.* **2004**, *121*, 3405−3416.
(43) Becke, A. D. *J. Chem. Phys.* **1996**, *104*, 1040−1046.
(44) Tao, J.; Perdew, J. P.; Staroverov, V. N.; Scuseria, G. E. *Phys. Rev. Lett.* **2003**, *91*, 146401.
(45) Grimme, S. *J. Chem. Phys.* **2006**, *124*, 034108.
(46) Karton, A.; Tarnopolsky, A.; Lamère, J.-F.; Schatz, G. C.; Martin, J. M. L. *J. Phys. Chem. A* **2008**, *112*, 12868−12886.
(47) (a) Perdew, J. P. In *Electronic Structures of Solids '91*, Ziesche, P., Eschrig, H., Eds.; Akademie Verlag: Berlin, 1991; p 11. (b) Perdew, J. P.; Chevary, J. A.; Vosko, S. H.; Jackson, K. A.; Pederson, M. A.; Singh, D. J.; Fiolhais, C. *Phys. Rev. B* **1992**, *46*, 6671−6687. (c) Perdew, J. P.;

Chevary, J. A.; Vosko, S. H.; Jackson, K. A.; Pederson, M. A.; Singh, D. J.; Fiolhais, C. *Phys. Rev. B* **1993**, *48*, 4978. (d) Perdew, J. P.; Burke, K.; Wang, Y. *Phys. Rev. B* **1996**, *54*, 16533−16539. (e) Burke, K.; Perdew, J. P.; Wang, Y. In *Electronic Density Functional Theory: Recent Progress and New Directions*; Dobson, J. F., Vignale, G., Das, M. P., Eds. Plenum Publishing: New York, 1998.

(48) Goerigk, L.; Grimme, S. *J. Chem. Theory Comput.* **2011**, *7*, 291−309.

(49) (a) Grimme, S.; Antony, J.; Ehrlich, S.; Kreig, H. *J. Chem. Phys.* **2010**, *132*, 154104. (b) Schwabe, T.; Grimme, S. *Acc. Chem. Res.* **2008**, *41*, 569−579. (c) Schwabe, T.; Grimme, S. *Phys. Chem. Chem. Phys.* **2007**, *9*, 3397−3406. (d) Grimme, S. *J. Comput. Chem.* **2006**, *27*, 1787−1799.

(50) Grimme, S.; Ehrlich, S.; Goerigk, L. *J. Comput. Chem.* **2011**, *32*, 1456−1465.

(51) (a) Johnson, E. R.; Becke, A. D. *J. Chem. Phys.* **2006**, *124*, 174104. (b) Johnson, E. R.; Becke, A. D. *J. Chem. Phys.* **2005**, *123*, 024101.

(52) (a) Szabados, Å. *J. Chem. Phys.* **2006**, *125*, 214105. (b) Grimme, S. *J. Chem. Phys.* **2003**, *118*, 9095−9102.

(53) Møller, C.; Plesset, M. S. *Phys. Rev.* **1934**, *46*, 618−622.

(54) Kozuch, S.; Gruzman, D.; Martin, J. M. L. *J. Phys. Chem. C* **2010**, *114*, 20801−20808.

(55) Perdew, J. P. *Phys. Rev. B* **1986**, *33*, 8822−8824.

(56) Kozuch, S.; Martin, J. M. L. *Phys. Chem. Chem. Phys.* **2011**, *13*, 20104−20107.

(57) Ernzerhof, M.; Perdew, J. P. *J. Chem. Phys.* **1998**, *109*, 3313−3320.

(58) Kozuch, S.; Martin, J. M. L. *J. Comput. Chem.* **2013**, *34*, 2327−2344.

(59) Martin, J. M. L., personal communication.

(60) It is assumed that standard DFT methods provide reasonable geometries for each spin state, even when the energy orderings are incorrect. While this is a reasonable assumption, it would be very hard to test.

(61) Gore-Randall, E.; Irwin, M.; Denning, M. S.; Goicoechea, J. M. *Inorg. Chem.* **2009**, *48*, 8304−8316.

(62) Biner, M.; Bürgi, H.-B.; Ludi, A.; Röhr, C. *J. Am. Chem. Soc.* **1992**, *114*, 5197−5203.

(63) Fogueri, U.; Kozuch, S.; Karton, A.; Martin, J. M. L. *Theor. Chem. Acc.* **2012**, *132*, 1291.

(64) Sorkin, A.; Iron, M. A.; Truhlar, D. G. *J. Chem. Theory Comput.* **2008**, *4*, 307−315.

(65) See, for example, (a) Reiher, M.; Salomon, O.; Hess, B. A. *Theor. Chem. Acc.* **2001**, *107*, 48−55. (b) Handy, N. C.; Cohen, A. J. *Mol. Phys.* **2001**, *99*, 403−412. (c) Reiher, M. *Inorg. Chem.* **2002**, *41*, 6928−6935. (d) Holthausen, M. C. *J. Comput. Chem.* **2005**, *26*, 1505−1518. (e) Ganzenmüller, G.; Berkaïne, N.; Fouqueau, A.; Casida, M. E.; Reiher, M. *J. Chem. Phys.* **2005**, *122*, 234321. (f) Zein, S.; Borshch, S. A.; Fleurat-Lessard, P.; Casida, M. E.; Chermette, H. *J. Chem. Phys.* **2007**, *135*, 014105. (g) Güell, M.; Luis, J. M.; Rodriguez-Santiago, L.; Sodupe, M.; Solà, M. *J. Phys. Chem. A* **2009**, *113*, 1308−1317. (h) Yang, K.; Peverati, R.; Truhlar, D. G.; Valero, R. *J. Chem. Phys.* **2011**, *135*, 044118. (i) Valero, R.; Illas, F.; Truhlar, D. G. *J. Chem. Theory Comput.* **2011**, *7*, 3523−3531. (j) Capano, G.; Penfold, T. J.; Besley, N. A.; Milne, C. H.; Reinhard, M.; Rittmann-Frank, H.; Glatzel, P.; Abela, R.; Rothlisberger, U.; Chergui, M.; Tavernelli, I. *Chem. Phys. Lett.* **2013**, *480*, 179−184.

(66) (a) Becke, A. D. *J. Chem. Phys.* **2013**, *138*, 161101. (b) Becke, A. D. *J. Chem. Phys.* **2013**, *138*, 074109.

(67) Becke, A. D., personal communication.